

UNIVERSIDADE DE LISBOA
FACULDADE DE CIÊNCIAS
DEPARTAMENTO DE FÍSICA



Characterisation of biological tissue:
measurement of acoustic properties for
Ultrasound Therapy

Sara Ferreira Reis

Dissertação
Mestrado Integrado em Engenharia Biomédica e Biofísica
Perfil de Sinais e Imagens Médicas

2013

UNIVERSIDADE DE LISBOA
FACULDADE DE CIÊNCIAS
DEPARTAMENTO DE FÍSICA



Characterisation of biological tissue:
measurement of acoustic properties for
Ultrasound Therapy

Sara Ferreira Reis

Dissertação
Mestrado Integrado em Engenharia Biomédica e Biofísica
Perfil de Sinais e Imagens Médicas

Orientadores: Professor Doutor Nuno Matela
Professor Doutor Nader Saffari

2013

Resumo

O fígado é um local frequente de ocorrência de tumores primários e secundários (do intestino, colo-rectal e cancro do estômago). A incidência de cancro do fígado a nível mundial é mais do que um milhão de casos por ano. O cancro no fígado mais comum encontrado na prática clínica são as metástases hepáticas que, juntamente com o carcinoma colo-rectal são os tipos histológicos mais predominantes. O cancro do fígado primário contribuiu com mais de 21 mil novos casos e causou 18.000 mortes nos Estados Unidos em 2008. O carcinoma hepatocelular (HCC) é o cancro primário de fígado mais comum, com uma incidência global estimada de mais de meio milhão de novos casos por ano e é a terceira maior causa de mortes por cancro em todo o mundo. Sem tratamento específico, o prognóstico é muito pobre, e as taxas de sobrevivência médias para pacientes com tumores iniciais e avançados são 6-9 meses e 1-2 meses, respectivamente. O HCC recorrente ocorre em 50% a 80% dos pacientes em 5 anos após a cirurgia de ressecção, a maioria ocorrendo no prazo de 2 anos. Após o tratamento para o HCC, 50% a 90% das mortes no pós-operatório é devido a doença recorrente.

A hepatectomia (ressecção hepática) é viável apenas em 10-20% dos casos, e está associada a uma mortalidade operatória de até 5%, no entanto pode atingir taxas de sobrevivência de 5 anos em cerca de 40%. A alternativa actual à cirurgia é a combinação com quimioterapia, mas esta está associada uma taxa de resposta de 20-50%, e taxa de sobrevivência global relativamente curta (12-18 meses). Como resultado, têm sido feitos esforços consideráveis no sentido de proporcionar uma alternativa minimamente invasiva à cirurgia para estes doentes. Essas alternativas actualmente incluem a ablação por radiofrequência, crioterapia e terapia com laser. A única terapia local proposta não-invasiva até à data é High Intensity Focused Ultrasound (HIFU). HIFU é um procedimento não-invasivo que por meio de uma fonte extracorpórea de ultra-sons de alta intensidade concentrada induz a necrose por coagulação total de um tecido alvo específico, sem necessidade de exposição cirúrgica ou a inserção de instrumentos no interior da lesão.

A intenção do tratamento por HIFU é elevar a temperatura de uma região

de tecido delimitada e isolada acima dos 55°C e manter essa temperatura durante 1 segundo ou mais. Isto, por sua vez induz a necrose por coagulação e morte celular. Os pequenos comprimentos de onda (mm) do ultra-som em frequências da ordem dos megahertz (MHz) em tecidos moles permitem que ele seja focado em pequenos volumes clinicamente relevantes. O perigo da maioria dos tratamentos ablativos, onde as células cancerígenas são destruídas pelo aumento da sua temperatura, é que o tecido saudável pode ser danificado. Com HIFU, a energia pode ser focada num volume muito pequeno e bem definido, fazendo com que a passagem do ultra-som através dos tecidos intervenientes, não cause nenhum efeito cumulativo aparente para esses tecidos.

HIFU foi aprovado para terapias clínicas de tumores sólidos ou para outras doenças do fígado, rim, pâncreas, recto, próstata, mama, osso, pele e do útero. Em vários centros no mundo, o HIFU está a ser utilizado clinicamente para o tratamento de tumores sólidos (tanto malignos e benignos), incluindo os da próstata, do fígado, da mama, do rim, do osso e do pâncreas, e sarcoma de tecido mole. Tanto o cancro de fígado primário (carcinoma hepatocelular) e metástases hepáticas de cancros do cólon e estômago já foram tratados com HIFU. Apesar dos sucessos clínicos iniciais com tratamentos extracorpóreos de tumores abdominais, ainda existem alguns limites a ultrapassar - especialmente no que diz respeito ao tratamento do fígado, pâncreas e rins - antes de esta técnica poder ser utilizada de forma segura e rotineiramente no interior do corpo. Outra dificuldade importante a ter em conta é o facto de o comprimento do percurso nos tecidos que sobrepõem estes órgãos ser longo e, em geral, a sua composição ser pouco homogénea.

Por exemplo, o tratamento terá que transmitir energia através da caixa torácica, o que pode aumentar o risco de queimaduras na pele e danos à superfície das costelas. Do mesmo modo, uma vez que o paciente respira, os efeitos desse movimento durante o tratamento precisa de ser explorado. Podem também ocorrer efeitos de cavitação como resultado do tratamento, e estes efeitos devem ser também considerados. Finalmente, actualmente ainda não existe uma técnica de imagem em tempo real completamente eficaz para a monitorização do tratamento, sendo este um requisito necessário para que a técnica seja utilizada e aplicada com sucesso. Para resolver estas questões, foi desenvolvido um projecto financiado pelo Engineering & Physical Sciences Research Council intitulado "THIFU - Trans-Costal High Intensity Focused Ultrasound" que tem como principal objectivo o desenvolvimento de uma nova técnica para a utilização de HIFU no tratamento de cancros na zona abdominal superior. O objectivo global do programa é desenvolver soluções práticas para esses problemas.

Um dos objectivos com o projecto THIFU é a optimização da ablação

do tecido no volume alvo e a minimização dos efeitos em estruturas críticas que sobrepõem o local onde queremos administrar a energia ultra-sónica, tais como a pele e a caixa torácica. O planeamento exacto do tratamento e o seu monitoramento bem como a própria administração do mesmo são fundamentais para isso.

A fim de melhorar o planeamento e a administração do tratamento, é necessária proceder a uma caracterização precisa das propriedades físicas do tecido. Para isso, é indispensável uma compreensão completa dos campos acústicos, das propriedades dos tecidos no caminho de propagação do ultra-som e os mecanismos pelos quais a destruição dos tecidos é induzida pelo feixe de HIFU. Desta forma, é também importante conhecer a interacção do feixe de ultra-som com os diferentes tipos de tecido, com o fim de criar com precisão um plano de tratamento para a entrega da energia ultra-sónica no foco desejado. Assim, um dos objectivos deste projecto é obter uma estimativa precisa das propriedades acústicas dos tecidos-alvo (por exemplo, a velocidade do som e o coeficiente de atenuação). Esta informação é depois utilizada para determinar a absorção de energia e de transmissão da energia ultra-sónica nos tecidos-alvo. Estes resultados serão usados como parâmetros input para o software de planeamento de tratamento desenvolvido no projecto THIFU.

O objectivo do trabalho descrito nesta dissertação foi abordar os desafios de medir as propriedades acústicas (velocidade do som, coeficiente de atenuação e o coeficiente de não-linearidade) dos tecidos moles - mais concretamente em amostras de fígado humano obtidas logo após uma hepatotomia - que são atravessados pelo feixe HIFU durante o tratamento, com um sistema “*all in one*” que permite avaliar estas propriedades numa única amostra e num curto espaço de tempo, evitando assim a degradação das amostras.

Foi feita uma investigação inicial com o intuito de validar o sistema *all in one* construído para o efeito com materiais considerados de referência (as suas propriedades acústicas são bastante conhecidas), como por exemplo *phantoms* em gel e óleo de rícino. Foram também recolhidos dados referentes a amostras de tecidos de origem animal e mais tarde procedeu-se à quantificação das propriedades acústicas de tecido hepático humano.

Os valores obtidos com um líquido de referência – óleo de rícino – medido no sistema *all-in-one* a 23°C estão de acordo com valores publicados por outros estudos.

Foram analisadas seis amostras de fígado humano de diferentes patologias. Um total de três tipos de tecidos foi estudado: saudável/normal, cancerígeno e cirrótico. Os resultados obtidos para as amostras de tecido de fígado humano, não mostram clara diferenciação entre o tumor e tecido normal e grande variação entre as amostras. Devido ao tamanho pequeno da

amostra não é possível retirar conclusões estatisticamente significativas e precisas nesta fase. No entanto, os resultados gerais mostram que o sistema all-in-one é capaz de determinar estes parâmetros em amostras de referência - como phantoms de criogel e amostras de óleo de rícino - amostras de tecido animal *ex-vivo* e de tecido hepático humano.

Trabalho futuro irá envolver a otimização de certos factores referentes aos materiais e métodos utilizados bem como melhoramentos nos protocolos de preparação das amostras, estudos adicionais com um tamanho de amostra maiores, estudo destas propriedades nos tecidos entre um intervalo de temperaturas relevante para a técnica de HIFU, etc.

A dissertação está dividida em 5 capítulos. O primeiro capítulo consiste numa introdução ao tema abordado e a descrição dos principais conceitos inerentes ao trabalho desenvolvido. O segundo capítulo descreve os materiais e metodologias utilizadas. No terceiro e quarto capítulo encontram-se descritos os principais resultados e as conclusões, respectivamente.

Palavras-chave: Cancro, High Intensity Focused Ultrasound (HIFU), Ultrassom, Propriedades Acústicas, Atenuação, Velocidade do Som, Não-linearidade

Abstract

High-intensity focused ultrasound (HIFU) provides a potential noninvasive alternative to conventional therapies. In spite of early clinical successes with extracorporeal treatments of abdominal tumours, there are some remaining challenges, especially related to access to the liver, pancreas and kidney.

This thesis addresses the challenges of measuring the acoustic (sound speed, attenuation and non-linearity coefficients) properties of soft tissues that lie within the HIFU beam during treatment. Differences in these tissue properties may affect the delivery of thermal therapies, but may also provide a basis for their monitoring with ultrasound. Novel measurement techniques have been developed and applied in the construction of an "all-in-one" tissue characterisation system that allows for the determination of all these parameters in the same region of a single sample.

The finite amplitude insertion substitution (FAIS) method was used to obtain the attenuation coefficient and speed of sound. Nonlinearity coefficients were measured using an adapted version of the FAIS method.

The attenuation coefficient, sound speed and the acoustic nonlinearity parameter B/A were determined for explant human liver tissue samples with different pathological characteristics. A total of three tissue types were studied: healthy/normal, tumorous and cirrhotic. The results obtained for the human liver tissue samples show no clear differentiation between tumour and normal tissue and big variation between samples. However, as a result of the small sample size and no clear pattern observed, it is not statistically possible to draw accurate and statistically significant conclusions at this stage.

The overall results show that the system is able to determine these parameters in reference samples such as cryogel phantoms and castor oil samples, animal ex-vivo tissue and explant human liver tissue. Future studies with a bigger sample size will be required in order to validate the system and also explore thoroughly the relationship between the acoustic properties and temperature variations in the tissue.

Keywords: Liver cancer, High Intensity Focused Ultrasound (HIFU),

Ultrasound, Acoustic properties, Coefficient of attenuation, Speed of sound,
Coefficient of non-linearity, B/A

Acknowledgments

Thank you first and foremost to my UCL supervisor Professor Nader Saffari who gave me the opportunity to work in this project. I thank him for his encouragement and guidance, for all the advice and dedication but also his kindness and great sense of humour.

I am extremely grateful to Dr John Civalé who developed the matlab interface and the code for the data processing and for his guidance and help with my experimental work with the characterisation system. I would like to extend my gratitude to Mr Richard Symonds-Tayler as he helped write some of the code to control the system hardware.

I am very thankful for the support and help of Professor Nuno Matela during my internship and for the dozens of recommendation letters he wrote to help me get my next challenge. I would also like to thank the research team at ICR – Professor Gail Ter Haar, Dr Ian Rivens and Vicky – and Professor Brian Davidson from Royal Free Hospital for having been part of the development of my project.

Thank you to everyone at the Department of Mechanical Engineering specifically Santiago, Reza, Kijoo and Laura and everyone in the Malet Place Building, you made my stay in London one of the best experiences of my life. A special thanks to Clément, Sofia, Dan, Ireneos, Zach, David, António and Tunder for the great moments we spent together, you will always be in my heart.

A big and warm thank you to my girls Andreia, Mónica and Tania, without you London would have never happened. Thank you for the intense, stressful, funny (and sometimes dreadful) moments in the last five years.

My profound gratitude to Joana, Verónica and Carolina, that even though we were separated by 1600 km you were always by my side.

Last but definitely not least my brother Pedro and my wonderful parents Sandra and Vitor. I owe you everything I am today, without your support and encouragement to always be at my best I wouldn't be half the person I am today.

Contents

Resumo	i
Abstract	v
Acknowledgements	vii
List of Figures	xii
List of Tables	xiii
List of Abbreviations	xiii
1 Introduction and Motivation	1
1.1 Introduction	1
1.2 Background and Motivation	1
1.3 Aim and Objectives	3
1.4 Thesis Structure	3
2 Theoretical Background	5
2.1 Literature Review	5
2.2 Ultrasound propagation through tissue	8
2.2.1 Attenuation	9
2.2.2 Speed of Sound	10
2.2.3 Non-linear Acoustics	10
2.3 Methods for measuring acoustic properties	13
2.3.1 Attenuation Coefficient	13
2.3.2 Speed of Sound	15
2.3.3 Non-linearity Coefficient	16
2.4 Thermal effects	16
2.4.1 Bio-Heat Transfer Equation	16
2.4.2 Thermal Dose	17
2.5 Published values of the acoustic properties of tissue	17

CONTENTS

2.5.1	Attenuation Coefficient	17
2.5.2	Speed of Sound	19
2.5.3	B/A coefficient	20
3	Materials and Methods for Acoustic Characterisation in Biological Tissues	21
3.1	All-in-one Tissue Characterisation System	21
3.2	Attenuation coefficient and Speed of Sound	25
3.2.1	Experimental Arrangement	25
3.2.2	Method for determining Attenuation Coefficient and Speed of Sound	25
3.2.2.1	Attenuation Coefficient	25
3.2.2.2	Speed of Sound	26
3.2.3	Data analysis	27
3.2.3.1	Post-processing	28
3.3	Non-linearity coefficient	32
3.3.1	Experimental Arrangement	32
3.3.2	Method for determining B/A coefficient	33
3.3.3	Data analysis	36
3.4	Experimental Protocols	38
3.4.1	Animal experiments	38
3.4.2	Human tissue experiments	39
4	Acoustic Properties of Human Liver Tissue	42
4.1	Validation Experiments	42
4.1.1	Cryogel phantoms	42
4.1.2	Reference liquids	43
4.1.2.1	Reference sample: Castor Oil	43
4.1.3	Characterisation of the second harmonic as a function of distance	45
4.2	Animal ex-vivo experiments	47
4.3	Human Liver Tissue	51
4.3.1	Attenuation and Speed of Sound	53
4.3.1.1	Normal Liver	53
4.3.1.2	Tumour tissue	53
4.3.1.3	Cirrhotic and Fatty Liver	55
4.3.2	B/A coefficient	56
4.3.3	Acoustic properties as a function of temperature	56

CONTENTS

5	Discussion and Conclusions	59
5.1	Animal samples	59
5.2	Human liver tissue	60
5.2.1	Acoustic properties as a function of temperature	62
5.3	Overall conclusions and Future work	63
	Bibliography	64
	Appendix	74
A	Matlab code	74
A.1	Second harmonic vs. distance data processing	74

List of Figures

2.1	The evolution of the shape of a sinusoidal wave in a non-linear, weakly and dispersively attenuating medium [37]	11
2.2	Experimental configuration for attenuation coefficient	14
2.3	Time of flight method	15
3.1	Schematic diagram of the tissue characterisation system.	22
3.2	Schematic of the configuration of the experiments	23
3.3	Matlab Interface	24
3.4	Schematic of the configuration of the experiments	25
3.5	Digitise pulses and Frequency dependent signals	27
3.6	Example of a the typical plots obtained with the code for the attenuation and speed of sound measurements.	28
3.7	Attenuation Coefficients maps for a castor oil sample	29
3.8	Frequency dependency fit parameters maps for a castor oil sample	30
3.9	Top: Thickness and Speed of Sound maps; Bottom: Front and Back window reflections maps	30
3.10	Attenuation coefficient maps at selected frequencies. Sample - human liver tissue	31
3.11	Experimental Arrangement for the B/A measurements	32
3.12	Diagram of the typical experimental set up	33
3.13	An example of the software during B/A measurement with a typical waveform.	37
3.14	Second Harmonic Ratio and B/A parameter maps.	37
3.15	Example of an ex-vivo animal sample preparation.	39
3.16	Example of an human liver sample preparation.	40
4.1	Measured attenuation coefficient versus frequency.	43
4.2	Castor oil sample.	44
4.3	Verification of the methods and equipment in the system using Castor Oil and comparison with literature values.	45

LIST OF FIGURES

4.4	Top Left: Signal received at the sensor; Top Right: 10-cycle pulse section of the signal received at the sensor; Bottom Left: Frequency spectrum of the 10-cycle section; Bottom Right: Distance between the transmitter and the receiver versus FFT of the Second Harmonic.	46
4.5	Extrapolation of the data to the transducer ($z=0$).	47
4.6	Comparison of the attenuation coefficient results for bovine ex-vivo samples obtained with the system and the literature values.	48
4.7	Comparison of the speed of sound values for bovine ex-vivo samples obtained with the system and the literature values. . .	48
4.8	Photographs, attenuation at 3 MHz and speed of sound maps of some samples.	52
4.9	Measured Attenuation coefficients for 3 samples in function of frequency.	53
4.10	Attenuation coefficient in function of frequency: comparison between healthy and tumorous samples.	54
4.11	Attenuation coefficient in function of frequency: tumour samples.	55
4.12	Measured Speed of sound values.	56
4.13	Attenuation maps at 3 MHz at 38°C and 50°C (from left to right)	56
4.14	Attenuation coefficients in function of frequency at 38°C and 50°C.	57
4.15	Speed of Sound maps at 38°C and 50°C (from left to right). . .	57
4.16	Measured Speed of Sound values at 38°C and 50°C.	57
4.17	B/A coefficient maps at 38°C and 50°C (from left to right). . .	58
4.18	Measured B/A coefficient values at 38°C and 50°C.	58

List of Tables

2.1	Published sound speed for human tissues	19
2.2	Published B/A coefficient for human tissues	20
3.1	List of the measurements done for each animal ex-vivo sample.	38
3.2	List of the measurements done in each specimen of human liver, specifying scans conditions	41
4.1	Acoustic properties measured of the reference media: cryogel .	43
4.2	Published Velocity and Attenuation coefficient for Castor Oil.	44
4.3	Acoustic properties of the reference media: degassed water and castor oil.	45
4.4	Measured attenuation coefficients in bovine and porcine liver tissue samples.	49
4.5	Measured speed of sound in bovine and porcine liver tissue samples.	49
4.6	Measured B/A coefficients in bovine and porcine liver tissue samples.	50
4.7	Published speed of sound and B/A coefficient values.	50
4.8	Ultrasonic properties measurements in different types of human liver.	51
4.9	Published values for B/A coefficient and Speed of Sound for human liver.	55

List of Abbreviations

FAIS Finite-Amplitude Insertion-Substitution.

HCC Hepatocellular carcinoma.

HIFU High Intensity Focused Ultrasound.

MHz Megahertz.

MRI Magnetic Resonance Imaging.

RF Radiofrequency.

THIFU Trans-Costal High Intensity Focused Ultrasound.

TOF Time-of-flight.

US Ultrasound.

Chapter 1

Introduction and Motivation

1.1 Introduction

This thesis is inserted in a UK Engineering & Physical Sciences Research Council (EPSRC) funded project entitled "THIFU - Trans-Costal High Intensity Focused Ultrasound". The aim of the project is to design a prototype clinical device for the safe and effective HIFU treatment of tumours located behind the rib cage (liver and kidney) for patient use. It is a multidisciplinary collaboration project between the department of Mechanical Engineering and the Centre for Medical Image Computing (CMIC) of University College London (UCL), the Institute of Cancer Research (ICR) and Oxford University.

This thesis is a continuation of the work done by Dr. Lise Retat and it investigates the acoustic properties of human tissue, in particular human liver tissue, with an "all-in-one" tissue characterisation equipment built in ICR.

In this chapter the overall project motivation is described, the aims and objectives of the thesis are introduced, and finally details of the structure of the present thesis are given.

1.2 Background and Motivation

The liver is a frequent site of occurrence for both primary and secondary tumours (from bowel, colorectal and stomach cancer). [62] Incidence of liver cancer worldwide is more than a million cases per year. Hepatic metastases continue to be the most common liver cancer encountered in clinical practice, with colorectal carcinoma being by far the predominant histological type. Primary liver cancer is projected to contribute more than 21,000 new cases and cause 18,000 deaths in the United States during 2008. Hepatocellular carcinoma (HCC) is the most common primary liver cancer, with an esti-

mated global incidence of over half a million new cases per year and it is the third leading cause of cancer-related deaths worldwide.[58] Without specific treatment, the prognosis is very poor, and the median survivals for patients with early and advanced tumours are 6-9 months and 1-2 months, respectively. Recurrent HCC occurs in 50% to 80% of patients at 5 years after resection, the majority occurring within 2 years. Following curative treatment for HCC, 50%-90% of postoperative death is due to recurrent disease.[47] Hepatic resection is only feasible in 10–20% and is associated with an operative mortality of up to 5%, but can achieve 5-year survival rates in the region of 40%. The favoured current alternative to surgery would be combination chemotherapy, but this is associated an objective response rate of 20–50%, and relatively short median overall survival rate of 12–18 months. As a result there have been considerable efforts to provide a minimally invasive alternative to surgery for such patients. Such alternatives currently include radiofrequency ablation, cryotherapy and laser therapy. The only non-invasive local therapy to be proposed to date is HIFU.[42]

HIFU is a highly precise, non-invasive procedure using a high-intensity, focused extracorporeal source of ultrasound to induce complete coagulative necrosis of a specific target tissue, without requiring surgical exposure or insertion of instruments into the lesion. The intention of a HIFU treatment is to raise the temperature of a selected, isolated tissue volume above 55 °C and to maintain this temperature for 1 second or longer.[73][64] This leads to coagulative necrosis and cell death. The short (mm) wavelengths of ultrasound at MegaHertz (MHz) frequencies in soft tissues allow it to be focused into small, clinically relevant volumes.[84] The danger in most ablative treatments, however, where tumour cells are destroyed by raising their temperature, is that surrounding healthy tissue can be damaged. Using HIFU, the energy can be focused into a very small and well defined volume, making the passage of ultrasound energy through the intervening tissues with no apparent cumulative effect on those tissues.[42]

HIFU has been approved for clinical therapies of solid tumours or other diseases in liver, kidney, pancreas, rectum, prostate, breast, bone, skin and uterus.[87] In several centres worldwide, HIFU is now being used clinically to treat solid tumours (both malignant and benign), including those of the prostate, liver, breast, kidney, bone and pancreas, and soft-tissue sarcoma.[43] Both primary liver cancer (hepatocellular carcinoma) and liver metastasis from colon and stomach cancers were treated using HIFU ablation.[1]

In spite of early clinical successes with extracorporeal treatments of abdominal tumours, there are some remaining challenges, especially related to access to the liver, pancreas and kidney. The path length in overlying tissues is long and in general, its composition is inhomogeneous.

One of the aims with the THIFU project is the optimisation of tissue ablation in the target volume, and minimisation of effects at critical overlying structures such as the skin and rib surface. Accurate treatment planning and monitoring, and control of treatment delivery are crucial to this.

In order to improve treatment planning and delivery, accurate characterisation of the physical properties of tissue is required, that including a thorough understanding of the acoustic fields, tissue properties in the ultrasound propagation path and the mechanisms by which tissue destruction is induced by the HIFU beam.

It is then important to know the interaction of the ultrasound beam with the different tissue types in order to accurately plan the delivery of the ultrasound energy to the right focus. Thus, it is necessary to obtain accurate estimates of tissue acoustic properties (e.g., speed of sound and attenuation) that will be used for determination of energy absorption and US transmission in the targeted tissues. These results will provide as input parameters for the treatment planning software developed in the THIFU project.

1.3 Aim and Objectives

The aim of the project is to perform quantification of acoustic properties of explant human liver tissue: attenuation coefficient, speed of sound and non-linearity coefficient. For each above the following has been carried out:

- Review of the published literature on human tissues relevant to HIFU treatment;
- Initial investigation of parameters, variables and practical problems using abattoir tissue followed by rigorous study of human tissues;
 - system validation experiments;
 - measurements of acoustic properties in known materials such as calibrated gels phantoms and reference liquids;
 - measurement of ex-vivo properties of abattoir tissue.
- Measurement of acoustic properties of explant human liver tissue samples with different pathological characteristics: healthy/normal, tumorous and cirrhotic.

1.4 Thesis Structure

Chapter 2 provides an introduction to the field of ultrasound and tissue characterisation using a description of the theoretical background and literature

CHAPTER 1. INTRODUCTION AND MOTIVATION

review.

Chapter 3 describes the techniques and methods used in the experiments along with the "all-in-one" equipment that allows the measurement of the parameters to be done in the same region of a tissue sample of interest.

The experiment results can be found in chapter 4 and the overall conclusions from the project and points to future work in chapter 5.

Chapter 2

Theoretical Background

2.1 Literature Review

The first work to consider potential applications of HIFU was published in 1942 by Lynn et al. [53]. They were the first to build and test a focused ultrasound transducer that produced focal heating in a certain area without injuring the intervening tissue. Fry et al. [27] [83] produced lesions in the brains of cats and monkeys. Later, Frank Fry treated patients with Parkinson's disease and other neurological conditions [24]. Using a set of ultrasound transducers focused on the area to be treated they were able to induce biological lesions located deep inside the cerebral cortex. The treatment was done invasively by exposing the dura under local anesthetic. The treatment proved to eliminate the symptoms, but it was not taken further into investigation.

In the 1970s, ultrasound was investigated for treating tumours at lower intensities. The aim was to cause hyperthermia in the tumour volume by maintaining a temperature of $\sim 43^\circ\text{C}$ for a certain time. [40] However, there were a lot of difficulties involved in the delivery. The lack of a method to monitorised the delivered acoustic energy to the tumour resulted in non-uniform heating and lack of maintenance the entire volume at a temperature greater than 43°C .

The specific properties of focused ultrasound conduction and modes of destruction in normal tissues were investigated further during the 1970s and 1980s.

Taylor et al. [70] showed that the effects of HIFU depended not only on the frequency, intensity, duration and form of the ultrasonic beam, but also on the absolute length of the pulses and of the intervals between them. He also described lesions due to the reflection of ultrasound waves at the liver-air interfaces.

Bamber et al. [6] studied the importance of temperature as a variable in determining the precision in vitro measurements of the ultrasonic propagation properties. He observed that at temperatures below 40 °C the attenuation coefficient behaved similarly for fixed and fresh tissues where, at high frequencies, it had a negative dependence on temperature. At temperatures above 40 °C, the attenuation coefficient of freshly excised tissues increased with temperature, whereas for fixed tissues the attenuation coefficient continued to decrease. He also observed that as the frequency is reduced, the temperature coefficient of attenuation progressively decreases until a positive dependence on temperature appeared. These observations were helpful in a way that was able to resolve a possible discrepancy evident in previous reports of the temperature dependence of attenuation. [14]

Frizzell [23] studied the threshold dosages for high-intensity focal lesion production to mammalian liver. Linke et al. [52] exposed rat liver and rabbit kidney and liver directly to an ultrasound transducer and observed a maximum lesion size the third day after the treatment, and its replacement by a thin fibrous scar after several months.

Studies using HIFU to irradiate experimental tumours followed. Fry and Johnson [25] investigated the destruction of tumours in an animal model using HIFU and found that survival rate increased for treated animals.

Goss et al. [32] studied the effects of high-intensity focused ultrasound in tumour growth and his results showed that reduction in tumour growth can be achieved. 35% of the animals treated presented non-palpable tumours up to 120 days post irradiation. Among the remaining animals, tumour volume was reduced by about 85% over those of shams (significance at $p \leq 0.001$).

Ter Haar et al. [74] demonstrated that liver tumors in a rat model could be destroyed by HIFU without regrowth.

Chapelon et al. [10] studied the effects of HIFU on kidney tissue in the rat and the dog. He showed that the lesions obtained in the rat kidney were either coagulating necrosis or a 'punched out' cavity by increasing the intensity and/or shortening the exposure time. In the canine experiments, he achieved a kidney lesion in 63% of the animals extracorporally. He concluded that the lesions were the result of a combination of cavitation and thermal effects, depending on the duration and frequency of the ultrasound bursts.

While the potential therapeutic value of HIFU has been demonstrated, understanding and controlling HIFU exposure *in vivo* has proved to be a challenge. The source of damage to cells from HIFU exposure is thought to be a combination of thermal and mechanical mechanisms, with the contribution of each depending on the exposure conditions.

Hill [38] developed an analytical model for predicting HIFU lesion size and shape considering only a thermal mechanism. The model assumes a Gaus-

sian approximation to beam shape in the focal region and predicts, for any such focal beam, the time delay to initiation of a lesion and the subsequent time course of growth of that lesion in lateral and axial dimensions, taking into account the effects of thermal diffusion and blood perfusion. Comparison of predictions with experimentally measured data demonstrated good agreement.

Damianou and Hynynen [16] produced another model using thermal dose as a predictor of lesion volume that also only considered thermal effects. The lesion size was calculated as a function of the HIFU sonication time, power, and transducer parameters, and the findings were validated by *in vivo* experiments performed in canine and rabbit thighs. The lesion size after the experiments matched well with calculated results.

Both the authors didn't consider the nonlinear wave propagation at high-power intensities.

Lee and Yoon [49] studied the quantification of the lesion volume as a function of HIFU parameters. The purpose was to predict the size of the thermal lesion in soft tissue during HIFU treatment and to examine the dependence of the size on the sonication and transducer parameters and on the tissue properties. The theoretical calculations were performed to predict the change in the lesion size as the sonication time was varied from 5 s to 20 s. The increase in lesion dimensions with changing sonication time was determined at a constant acoustic intensity of $400\text{W}/\text{cm}^2$. They concluded that the lesion size could be controlled by adjusting the acoustic intensity, pulse duration, and frequency applied to the tissue. They also predicted that the lesion size did not strongly depend on either the perfusion rate or the attenuation coefficient of the tissue.

Wang et al. [80] performed *in vivo* studies on mice to investigate the damaging effect of HIFU on cancer cells and the inhibitory effect on tumor growth. The relationship between the death rate of cancer cells and HIFU sonication time as well as acoustic intensity was quantified.

Li et al. [50] studied the effects of acoustic intensity and sonication time on the lesion size by numerical calculations using O'Neill's equation and the bio-heat transfer equation. In these studies, HIFU ablation experiments were performed using excised bovine liver samples, and the lesion size was determined by dissecting the liver samples across the lesions after the experiments. The numerical and experimental results were compared and found to differ by as much as 20% at higher sonication times.

The response of the biological tissue to ultrasound exposure can be variable and depends on the acoustic and thermal properties as well as on the location and function of the exposed tissue. It is necessary to obtain accurate values of tissue acoustic and thermal properties that will be used for deter-

mination of energy absorption and US transmission in the targeted tissues. A comprehensive review of acoustic and thermal parameter values can be found in Duck [20] and Hill et al. [37].

2.2 Ultrasound propagation through tissue

The material presented here was obtained from text books such as Szabo [67] and Hill et al. [37] and review articles from ter Haar et al.[35].

Ultrasound is a pressure wave of frequency higher than 20 kHz or 20000 cycles per second. For medical applications frequencies typically above 1 MHz are used. Ultrasound propagation characteristics at these frequencies are particularly interesting. It is possible to predict the way which ultrasound propagates and interacts with the tissue by knowing of the wave properties, such as velocity, absorption, attenuation or reflection.

Ultrasound propagates as a longitudinal wave, where the molecules oscillate sinusoidally within the medium, moving forward and backward along the direction of propagation.

Alternatively the particles may oscillate transversely, perpendicularly to the direction of propagation. Such a wave is termed a transverse or shear wave. Though shear waves can propagate in solids, and may therefore travel in calcified tissues such as bone or tooth, they are of little relevance in soft tissue, which can barely support them at ultrasonic frequencies.

Within the wave, regular pressure variations occur with alternating areas of Compression, which correspond to areas of high pressure and high amplitude, and with areas of Rarefaction or low pressure zones where widening of particles occurs.

Ultrasound can be generated by a number of phenomena, however piezoelectric effect is of major importance when dealing with diagnostic applications.

The frequency f of a longitudinal wave is related to the speed of sound in the material, c , and its wavelength, λ , by the equation

$$c = \lambda f \quad (2.1)$$

Ultrasound interactions are determined by the acoustic properties of matter. As ultrasound energy travels through a medium, a multiple tissue layers for example, interactions that occur include reflection, refraction, scattering, and absorption before reaching to the desired target site.

At each tissue interface the energy carried by the wave will suffer reflection. When the incident beam is perpendicular to the boundary, a portion of

the beam (an echo) returns directly back to the source, and the transmitted portion of the beam continues in the initial direction.

The transmission coefficient depends primarily on the difference in acoustic impedance, Z that is defined by the product of the mass density and the speed of sound:

$$Z = \rho c \quad (2.2)$$

At interfaces where there is little difference in acoustic properties, the transmission coefficient is close to unity. With the exception of fat, air and bone, most tissues in the human body have acoustic properties similar to those of water. Aqueous media are therefore optimal for transmitting ultrasound energy from the transducer into the body, and reflections at tissue interfaces are generally weak.

2.2.1 Attenuation

When an ultrasonic wave propagates through tissue the effects of scattering and absorption contribute to the reduction in acoustic pressure amplitude that is, for attenuation generated by the tissue.

The loss of incident acoustic energy on a medium is characterised by its attenuation coefficient which can be defined as the sum of the absorption coefficient μ_a and the scattering coefficient μ_s :

$$\mu = \mu_a + \mu_s \quad (2.3)$$

The attenuation coefficient can be used to describe the loss of exponential intensity I during propagation through a distance x :

$$I = I_0 e^{-\mu x} \quad (2.4)$$

where I_0 is the non attenuated intensity.

For the majority of tissues, the attenuation coefficients depend on the frequency of the wave. This is explain by the fact ultrasound attenuation by a medium increases with the frequency in a way that the attenuation coefficient can be described via a power law:

$$\mu(f) = \alpha f^n \quad (2.5)$$

where α is the attenuation coefficient (*neper/cm/MHz*), f is the frequency (in *MHz*) and n is a material-dependent parameter.

2.2.2 Speed of Sound

The speed at which an ultrasonic wave propagates is controlled by the mechanical properties of the medium. For liquids and soft tissues the speed of the wave, c_0 , depends on the compressibility and the undisturbed density ρ_0 . Solids support both longitudinal waves and shear waves, whose speeds depend on the elastic moduli of the solid. However, simple equations are difficult to apply directly to biological solids, including bone. This is partly because the mechanical properties of some tissues depend on direction, and consequently so do their ultrasonic properties. This dependence on direction is termed anisotropy.

2.2.3 Non-linear Acoustics

Non-linearity is a property of the medium in which the shape and amplitude of the signal at a specific location is no longer proportional to its input. This produces behaviours that can't be predicted by an usual linear viewpoint.

Linear approximations are used to simplify, however non-linear approximations are more accurate but more difficult to simulate. As non-linearity effects are amplitude dependent they are usually called finite amplitude, as opposed to linear theory which is based in infinitesimal amplitudes.

If we assume a linear wave propagation, we can describe the equation of state for infinitesimal amplitudes as followed,

$$P = P_0 + A \left[\frac{\rho - \rho_0}{\rho} \right] \quad (2.6)$$

where

$$A = \rho_0 \left[\frac{\partial P}{\partial \rho} \right]_{0,S} = \rho_0 c_0^2 \quad (2.7)$$

This assumption allow us to eliminate the higher order terms in the Taylor series expansion because it is assumed that the particle oscillations associated with the propagation of the acoustic waves are small. If the amplitude of the wave is sufficiently great, this assumption is no longer valid.

For an acoustic wave of finite amplitude travelling in an isotropic medium the equation of state can be expressed by the Taylor expression

$$P = P_0 + A \left[\frac{\rho - \rho_0}{\rho} \right] + \frac{B}{2} \left[\frac{\rho - \rho_0}{\rho} \right]^2 + \dots \quad (2.8)$$

where

$$B = \rho_0^2 \left[\frac{\partial^2 P}{\partial \rho^2} \right]_{0,S} \quad (2.9)$$

P and P_0 are the instantaneous and hydrostatic pressures respectively, ρ and ρ_0 are the instantaneous and equilibrium densities respectively, and c_0 is the infinitesimal sound velocity. The partial derivatives are all evaluated in the unperturbed state p_0, s_0 , s being the specific entropy.

The coefficients A and B depend only on the properties of the medium, and may be expressed in terms of measurable entities.

The quantity B/A is proportional to the ratio of coefficients of the quadratic and linear terms in the Taylor series. Consequently it characterises the dominant finite-amplitude contribution to the sound speed for an arbitrary fluid. Its effect on the propagation speed of a progressive plane wave is manifest through the coefficient of non-linearity $\beta = 1 + B/2A$. [36] The B/A ratio is thus frequently used to characterise the non-linearity of the medium.

There are many consequences of acoustic propagation in a non-linear medium such as cumulative pulse and beam distortion, harmonic generation and saturation.

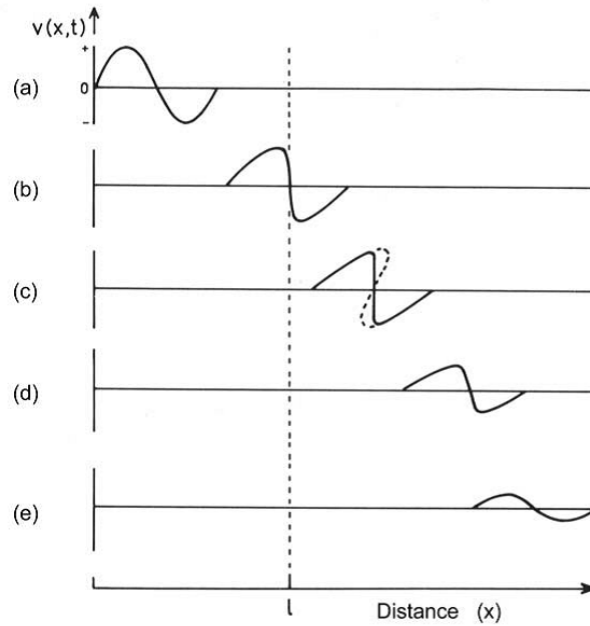


Figure 2.1: The evolution of the shape of a sinusoidal wave in a non-linear, weakly and dispersively attenuating medium [37]

A sinusoidal pressure wave with finite amplitude does not conserve its shape as it propagates through the medium. Figure 2.1 illustrates the progressive change of the shape of a sinusoidal wave in a non-linear medium. As the wave propagates through the medium, distortion begins to occur because the compressional phase velocity is greater than that in the rarefactional

phase and that creates low levels of harmonics.

As it spreads through a sufficient distance, the cumulative distortion leads to a 'sawtooth' waveform or a 'shock wave'. This wave has high frequency components that are multiples of the fundamental. Those components are attenuated more rapidly causing dissipation of these high frequencies, letting the wave with lower amplitude. As the distance increases and at higher frequencies, only a low-amplitude wave is left that is no longer proportional to the original sinusoidal wave.

The explanation for this progressive change in shape lies in the variation in phase speed v_t at different points on the wave. The phase speed is highest in the high-density compressions, and lowest in the low-density rarefactions.

The change in the shape of a wave that is initially of the form $u(0, t) = U_0 \sin(\omega t)$ is described by the following equation:

$$u(0, t) = U_0 \sin \left[\omega t - \frac{\omega x}{c_0} + \frac{x}{l} \frac{u}{U_0} \right] \quad (2.10)$$

and can be expressed in terms of a Fourier series expansion:

$$u = 2U_0 \sum_{n=1}^{\infty} \frac{J_n(nx/l)}{(nx/l)} \sin n(\omega t - \omega x/c_0) \quad (2.11)$$

where l is a constant that depends on the non-linear properties of the medium. This equation is only valid when $x < l$ and indicates that as the wave propagates, the energy of fundamental component is transferred to the other harmonics.[7]

The amount of non-linear distortion increases with a series of factors such as the frequency and amplitude of the wave, the non-linearity coefficient of the medium and the distance travelled by the wave.

At distances z , the distortion of the wave can be described by the shock parameter σ :

$$\sigma = \varepsilon \kappa \beta z \quad (2.12)$$

where ε is the acoustic Mach number, κ is the wave number and β is the coefficient of nonlinearity which is equal to $1 + B/2A$. Rewriting the expression we have:

$$\sigma = \frac{2\pi}{\rho_0 c_0^3} [p_0 f z (1 + B/2A)] \quad (2.13)$$

where p_0 is the acoustic pressure at the source and ρ_0 is the density.

For low values of σ , considerably less than 1.0, the magnitude of the second harmonic increases with the square of the acoustic pressure in the fundamental. The third and higher harmonics increase similarly, according

to the power of the harmonic number, n . As σ increases (e.g., with distance or amplitude), the amplitude of the fundamental decreases and those of the harmonics increase. With the eventual formation of a saw-tooth waveform at $\sigma = 3$, the harmonic amplitudes depend on $1/n$. [21]

2.3 Methods for measuring acoustic properties

2.3.1 Attenuation Coefficient

Many methods devised for making measurements of ultrasonic attenuation in a variety of media but only a few are suitable for the study of tissues at medical frequencies.

Fresh approaches to the measurement of attenuation have appeared.

Attenuation measurement techniques can be classified either as narrow-band or as broadband. For each class, it will be described the ones who are more relevant to the work reported here.

In narrowband techniques the transmitted acoustic signal is assumed to contain a sufficient number of cycles of the wave such that the measurement is regarded as being made at a single frequency.

In the class of pulse transmitted techniques we can make a distinction between "fixed path" and "variable path" methods. The path between the transmitter and the receiver may or may not be the same as the sound path through the specimen. Short bursts of sound are transmitted through the sample and received either by a another transducer aligned coaxially with the transmitter or by the same transducer after the pulse has been reflected by a plane interface and propagated back through the specimen.

Using pulses instead of a continuous signal allows the elimination of standing waves, multiple echoes and heating of the sample due to absorption.

When a variable path method is used, the value of α is obtained by the rate of change in the logarithm of the amplitude of the received signal with the position of the receiver or reflector. This method is independent of any coefficients of reflection or electromechanical transduction. However, it requires corrections for diffraction losses and it is not suitable for measurements on tissues.

For the fixed path pulse transmission methods, that includes the substitution method and the insertion technique, diffraction corrections are low and alignment tolerances less stringent comparing to the other technique available, however the measurements of the attenuation are done with relation to the attenuation coefficient of a reference liquid.

The substitution method has the transmitting and receiving transducers to move simultaneously, one through the reference liquid and the other through the test liquid with an acoustically transparent window separating the two liquids. In this way, α is determined independent of reflection coefficients because only the acoustic paths lengths between the two liquids are varied.

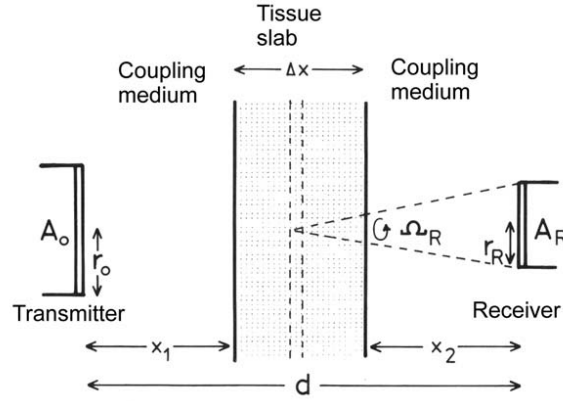


Figure 2.2: Experimental configuration for an attenuation measurement using the insertion technique. [37]

The insertion technique is more suited for studying solid tissues. The experimental configuration of this method is illustrated in Figure 2.2. The principle is the determination of the logarithm of the ratio of the received signals when the tissue is present between the transmitter and receiver and when it is only present a reference medium. The disadvantages of this method are the reflections at the specimen faces that are included in the measured loss and the fact that precise cutting of a parallel-sided tissue samples is very difficult to obtain.

A variety of methods were developed using a broadband transmitted acoustic signal with signal processing in the receiver to obtain α as a continuous function of frequency. It is easy to set up an automated system for spectral approach. In all broadband techniques, the tissue sample is examined using an insertion method. Practically what happens is that sound waves are converted upon reception to a spectrum of transmitted acoustic frequencies and the variation of α with frequency is determined from the logarithm of the ratio of the spectra obtained when tissue is in the path of the beam and when it is absent.

Then, the frequency analysis is generally done by first digitising the pulse in order to save the phase information and then computing the spectrum by means of a discrete Fourier transform algorithm.

A reference spectrum is obtained by using an acoustic reflector carefully aligned to be perpendicular to the beam axis. A tissue sample is then inserted between the transducer and the reflector and a new spectrum is obtained of the signal after a round-trip through the material. The difference of the two spectra yields twice the attenuation of the sample. If a broad band pulse is used, the attenuation over a range of frequencies is obtained.

2.3.2 Speed of Sound

The speed of sound is a property that is easy to measure with reasonable levels of precision over the frequency range of medical interest. Usually, when measuring speed of sound the system used is equal to that used for an associated attenuation measurement.

We can differentiate two types of methods: absolute and relative measurements methods. Both techniques are based on the time-of-flight (TOF) measurement [61]

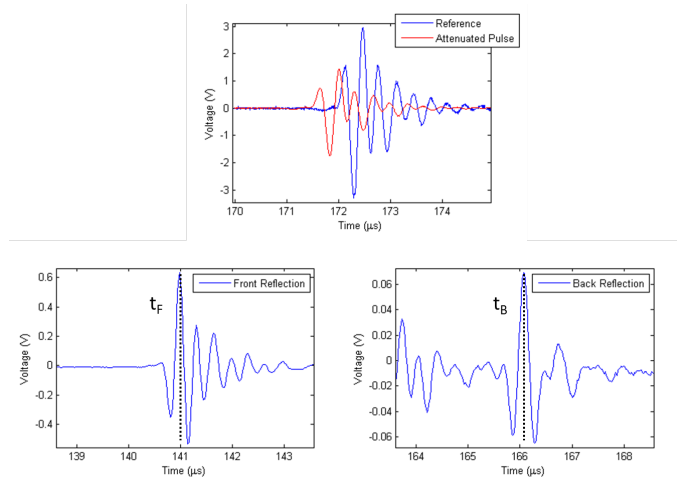


Figure 2.3: Time of flight method. Top: Representation of a reference waveform and its attenuated pulse; Bottom: Left - Front reflection signal (t_F is the pulse-echo time from the front window); Right - Back reflection signal (t_B is the pulse-echo time from the back window)

For absolute measurements the speed of sound is obtained from the difference in round-trip transit times as the path length between the transmitting transducer and a receiving transducer/ plane reflector is varied. If instead of a varied path we have a fixed path length, a single transit time or the transit times of multiple reflections between the two planes may be considered.

Absolute measurement methods allow direct measurement of sound speed in a medium of interest, without the need for a known characterised reference medium. As it is difficult to measure the length of the path or to vary it in solid samples, these methods aren't generally used for that objective.

Relative methods rely on the use of reference mediums in the measurement scheme thus, making the accuracy of the method dependent of the accuracy of the measurement of reference's absolute speed of sound value. A way to do this is simply using the TOF technique described above.

2.3.3 Non-linearity Coefficient

There are several methods for measuring the non-linearity parameter B/A in biological media. There are two main methods for determining the parameter B/A: the Thermodynamic method [89] [65] and the Finite Amplitude Insertion Substitution method (FAIS) method [30].

The thermodynamic method requires the measurement of the rate of change with ambient pressure of sound speed in the sample when the pressure is decreased rapidly enough to approximate an adiabatic depressurisation whereas the finite amplitude method is based on the measurement of the second harmonic generated during propagation of a sinusoidal wave.

2.4 Thermal effects

The material presented here was obtained from text books such as Szabo [67] and Hill et al. [37] and review articles from ter Haar et al.[35].

2.4.1 Bio-Heat Transfer Equation

The Bio-Heat Transfer Equation (BHTE) describes the rate of temperature change with time. This rate is dependent on the sum of terms that describe localized thermal diffusion, heat deposition and heat loss due to blood perfusion,

$$\rho C_t \frac{\partial T}{\partial t} = k \nabla^2 T + Q + WC_b(T - T_a) + M \quad (2.14)$$

where T is tissue temperature, T_a is arterial blood temperature, ρ is the tissue mass density, C_t and C_b are the tissue and blood specific heat capacities, Q is the heat deposition source, k is the tissue thermal conductivity, t is time and M is the heat generated by metabolic processes.

2.4.2 Thermal Dose

When a sound wave is propagated through an attenuation material like tissue, the amplitude of the wave is compromised. As said in section 2.3.1, attenuation is due to absorption and scattering. Absorption represents the portion of the wave energy that is converted into heat in the tissue, causing a temperature increase as long as the rate at which heat is produced is greater than the rate at which heat is dissipated.

It does not exist a specific definition of thermal dose for HIFU, however there is an empirical formula based on a hyperthermia study that relates the time t required to produce cell death to the time t_{43} that would be required for the exposure to caused tissue necrosis at a reference temperature of 43 °C. The thermal dose t_{43} : is define as

$$t_{43} = \sum_{t=0}^{t=final} \Delta t R^{(43-T)} \quad (2.15)$$

where t is time, T if for the temperature and R is a temperature-dependant constant where

$$R = \begin{cases} 0.5, & T > 43^\circ\text{C} \\ 0.25, & T \leq 43^\circ\text{C} \end{cases}$$

This has been shown to be valid up to about 50 °C, but for temperatures above that it may not apply.

2.5 Published values of the acoustic properties of tissue

2.5.1 Attenuation Coefficient

Several studies were taken over the years in measuring the attenuation coefficient of various soft tissues.

Attenuation changes with temperature appear to be more pronounced at temperatures above 50°C than in the hyperthermia range. In a study of inter-costal tissues from rats and pigs by Towa et al. [76], there was a statistically significant, but slight, change in attenuation coefficient from 22–37°C. They concluded that attenuation measures at 22° C, rather than at body temperature, were sufficient for accurate estimates of acoustic levels at pleural surfaces. Several groups have investigated the temperature dependence of tissue characteristics at temperatures above 50°C. [85] [15] [71] In measurements of insertion loss at room temperature before and after heating,

increases in attenuation of up to 2.4 dB cm^{-1} at 3.5 MHz were found in porcine liver after heating to 80°C in 300 s.[15]

Damianou et al. [17] investigated the temperature and frequency dependence of ultrasonic attenuation and absorption in soft tissues. They found that attenuation was highly dependent on temperature, but only at temperatures higher than 50°C .

Techavipoo et al. [71] measured attenuation of canine tissue from $25\text{--}95^\circ\text{C}$ with different tissue samples heated to different target temperatures to reduce cumulative tissue degradation. They found that attenuation at 3, 4 and 5 MHz was relatively unchanged from $40\text{--}60^\circ\text{C}$, but increased sharply above 60°C .

Ribault et al. [63] also looked at the effect of temperature rise on frequency-dependent attenuation and found that tissue damage (lesion formation) caused a change in attenuation in porcine liver *in vitro*. This effect was found by looking at the backscattered signal over the volume of the lesion and comparing the power received before and after high intensity focused ultrasound (HIFU). Thus, attenuation is of interest for thermometry, but probably only at temperatures above 50°C . This range, however, is not suitable for clinical hyperthermia because hyperthermia temperatures usually do not exceed 50°C .

Research has been done to look for possible correlations between liver pathology and attenuation coefficient changes.

Bamber and Hill [4] measured attenuation as a function of frequency in specimens of excised human liver to establish if it was possible to correlate variations in attenuation with the pathology and structure of the tissue. Their study showed that livers containing malignant disease possess different ultrasonic properties, however lack of sufficient data available prevented further conclusions.

Maklad *et al.* [54] performed attenuation measurements *in-vivo*. Their measurements were not corrected for diffraction effects which could have made their results biased, however various conclusions were made.

They stated that attenuation coefficients were higher in alcoholic cirrhotic livers (0.8 dB/cm/MHz), while in some cases of diffuse liver disease (0.56 dB/cm/MHz) the values remained within the normal range ($0.5 - 0.6 \text{ dB/cm/MHz}$). The attenuation coefficients in the livers of lymphoma and leukaemia patients were found to be low, and patients suffering from chronic active hepatitis also had lower liver attenuation coefficient estimates. They didn't find any correlation between collagen content and attenuation, which agreed with reports made by Bamber et al. [4]. They also showed that fat content was correlated with an increase in attenuation coefficient. Taylor *et al.* [68] also showed that the presence of fat was correlated the increase of

attenuation.

Parker *et al.* [59] found a significant correlation between high values of attenuation and ingestion of alcohol, chemotherapeutic agents, and steroids. Tuthill *et al.* [77] reported *ex-vivo* studies on rats and *in-vivo* studies on normal human before and after fasting. The results showed a statistically significant difference in liver attenuation between well fed and fasted individuals (greater than 10%). Clarke *et al.* [15] and Gertner *et al.* [29] showed that considerable tissue attenuation increases occur following prolonged heating.

2.5.2 Speed of Sound

The speed of ultrasound propagation in soft tissues is thought to have a mean value of 1540 m/s [82]. Moreover, the variation in the speed of ultrasound around this mean value is rather small, on the order of $\pm 5\%$.

The speed of sound in fat is at the low end of the spectrum (1460 m/s) [8][44] while in muscle it has been reported to be in the range 1550-1640 m/s [8][44][3].

In Table 2.1 are shown literature values for the speed of sound of several soft tissues. Data for pathological tissue are quite rare in literature, with some exceptions decribed in [78] and [5].

Lin *et al.* [51] The speed of sound in normal and diffusely-diseased liver specimens was measured. no significant correlation was found between speed of sound and fibrosis score; a moderate correlation was found between speed of sound and tissue water content; and a relatively good correlation ($r = -0.670$, p less than 0.1%) was found between the speed of sound and the histological fat score, which increased to $r = -0.819$ (p less than 0.1%) when a correction for variations in water content was used.

Table 2.1: Published sound speed for human tissues. [20]

Tissue	Temp ($^{\circ}\text{C}$)	c (m/s)
Blood	37	1560 – 1660
Fat/ fatty tissue	37	1427 ± 12.7
Breast	38	1553 ± 3.5
Liver	37	1578 ± 2.9
Kidney	37.2	1560 ± 1.8

Bush *et al.* [9] examined the acoustic appearance of lesions generated by high intensity focused ultrasound in excised pig livers. The results demonstrated significant increases in attenuation coefficient and sound speed in lesioned liver relative to normal.

Techavipoo *et al.* [72] performed measurements of the ultrasonic propagation speed and attenuation in tissue in vitro at discrete temperatures ranging from 25 to 95°C for canine liver, muscle, kidney and prostate. They found that in the 25–40 °C range, the speed of sound increases rapidly with temperature. Between 40–70 °C range it increases moderately with temperature, and it then decreases with increasing temperature from 70–95 °C.

2.5.3 B/A coefficient

Table 2.2 shows some B/A values taken from literature. Extensive literature on the determination of the acoustical nonlinear parameter in materials exists where studies were performed in both solids and fluids.

Table 2.2: Published B/A coefficient for human tissues. [20]

Tissue	Temp (° C)	B/A
Blood	26	6
Fat/ fatty tissue	37	9.63
Breast	37	10.25 ± 0.34
Glad bladder	26	6.22
Liver	37	6.75 ± 0.14

Seghal *et al.* [65] reported a temperature coefficient for B/A for human liver in the range 20 – 37 °C and observed an increase of the B/A within that temperature range. They measured fat and water composition of liver samples to establish a correlation with acoustic parameters at different temperatures. Both sound speed and B/A enables chemical composition to be estimated in terms of the volume fractions of water, fat and residual components such as protein and carbohydrates.

Zhang and Dunn [88] investigated the acoustic nonlinearity parameter for pathological porcine tissues in order to find the relation between this parameter and the pathological status of tissues. Their results indicated that all diseased tissues higher B/A values than corresponding normal tissues.

Chapter 3

Materials and Methods for Acoustic Characterisation in Biological Tissues

This chapter describes the techniques and methods used in the experiments along with the "all-in-one" equipment that allows the measurement of the acoustic parameters to be done in the same region of a tissue sample of interest.

3.1 All-in-one Tissue Characterisation System

This section describes in detail the all-in-one tissue characterisation system that was used for the measurements. The design of the all-in-one acoustic measurement system is represented in Figure 3.1. The system was built to allow acoustic measurements crucial for treatment planning - attenuation, non-linearity and speed of sound, to be made easily in the same specimen, sufficiently fast for the acquisition of good histological information and sufficiently compact for use in hospital environments where space may be restricted.

The system is comprised of two parallel adjacent measurements systems laterally separated. On one side, attenuation coefficient and speed of sound measurements are carried out. On the other, B/A determination is performed.

The FAIS method is used to estimate attenuation coefficient and speed of sound by using a pair of 2.5 MHz weakly focused transducers (6364A101, Imasonic, Besancon, France), aligned coaxially and confocally as a transmitter-receiver pair.

CHAPTER 3. MATERIALS AND METHODS FOR ACOUSTIC CHARACTERISATION IN BIOLOGICAL TISSUES

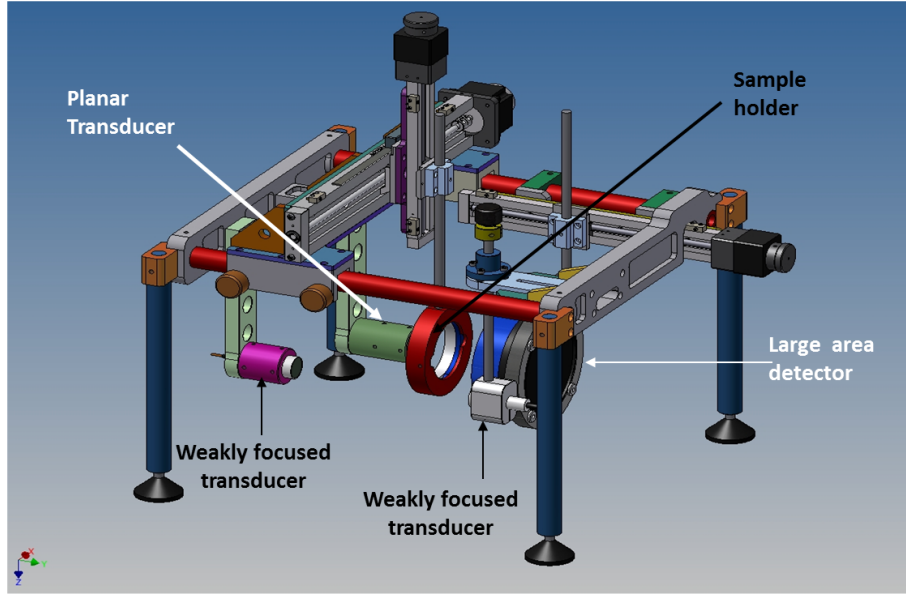


Figure 3.1: Schematic diagram of the tissue characterisation system. Done by Mr Chris Bunton[62]

For the B/A coefficient, the system consists in a 1 MHz planar transducer (PA347, Precision Acoustics, UK) and a pvdf membrane hydrophone with a 30 mm diameter sensor (Precision Acoustics, UK) tuned to be most sensitive at 2.0 MHz by use of 110 μm thick polyvinylidene difluoride (PVDF) film.

The two separated systems are aligned to acquire the measurements at identical positions in the sample. The systems and the sample holder are mounted on motorised gantries allowing measurements in different positions of the sample in a more accurate way.

The entire system is controlled via a Matlab interface developed by Dr. John Civalé. The interface is represented in Figure 3.3. As we can see from the Figure, we can control a variety of scan parameters. Before starting any measurement, the following parameters need to be set:

- **Grid Size:** where it is defined the area of the sample that will be analysed.
- **Step Size:** this is specified from a range of values in units of mm.
- **Offset:** sometimes the sample is not mounted properly at the center of the holder, or we are interested in a specific part of the sample, in these situations it is possible to do an offset correction.

CHAPTER 3. MATERIALS AND METHODS FOR ACOUSTIC CHARACTERISATION IN BIOLOGICAL TISSUES

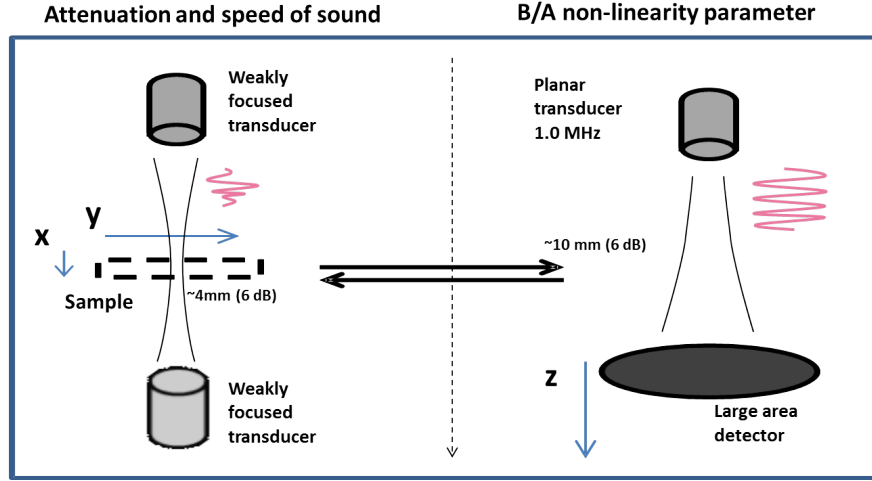


Figure 3.2: Schematic of the configuration of the experiments for the attenuation coefficient and speed of sound (left) and non-linear parameter (right)

- **Pulse Averages:** to increase the signal-to-noise-ratio. It allows select values of 1, 10, 100 and 1000 for the pulse averages.
- **Holder Windows:** depends on which holder is to be used. It can be either thin or thick mylinex (approximate thickness of 19 and 70 micrometers, respectively) membrane or none.
 - For attenuation and thickness/SOS measurements:
 - * Mylinex (thin and tick) and none - pulse-echo mode data is used to calculate thickness
 - * Membrane - allows user to override the pulse-echo thickness measurement by using the value specified in the thickness yellow box – this is desirable for situations where the pulse-echo measurement may not work accurately for example a very thin sample (a few mm, hence "membrane") or where the sample is badly mounted or gives poor front and back surface echoes.
 - For B/A measurements:
 - * Window amplitude transmission coefficients are changed depending on material [fundamental, second harmonic]:
 - Thin mylinex: $T=[0.99935 \ 0.99674]$;
 - Thick mylinex: $T=[0.98884 \ 0.95519]$;

CHAPTER 3. MATERIALS AND METHODS FOR ACOUSTIC CHARACTERISATION IN BIOLOGICAL TISSUES

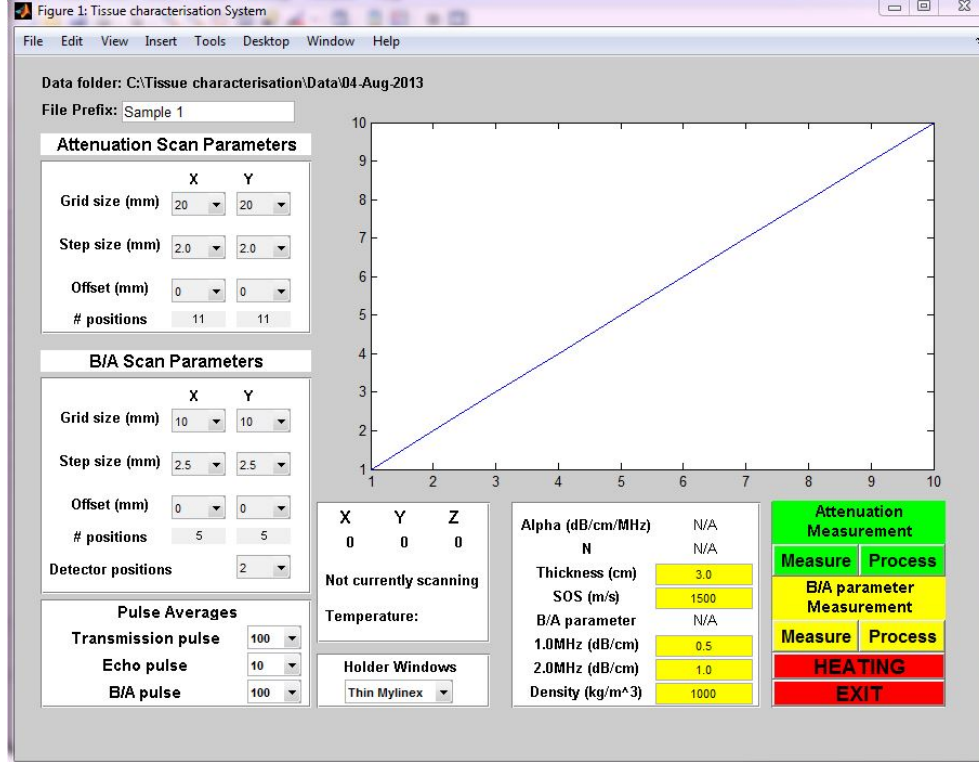


Figure 3.3: Matlab Interface

- Membrane and none: $T = 2*Z2/(Z1+Z2)$; where $Z1$ and $Z2$ are the respective acoustic impedance of the two materials, hence this depends on the measured sound speed in the sample

Depending on the grid size and step size chosen, the scan will be either quick with low resolution or it will take longer at higher resolution. The compromise between the resolution and the speed of the process depends on the purpose of the experiments and the type of samples. If we want to do analysis of the properties at different temperatures, it will be wiser to choose parameters that will result in a quicker analysis, for example.

In B/A scan parameters section we can define the number of positions that the detector will be at during the scan, this will be later explained.

3.2 Attenuation coefficient and Speed of Sound

3.2.1 Experimental Arrangement

The experimental arrangement for the measurement of attenuation coefficient and speed of sound is shown in Figure 3.4. The system comprises two weakly focused transducers (10 cm radius of curvature, 2 cm diameter - 6364A101, Imasonic, Besancon, France), aligned coaxially and confocally as a transmitter-receiver pair.

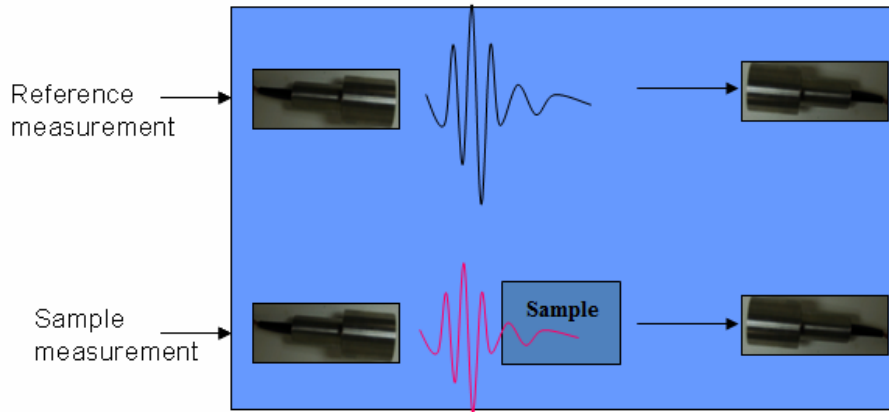


Figure 3.4: Schematic of the configuration of the experiments for the attenuation coefficient and speed of sound. [62]

The transmitting transducer is excited by a high voltage impulse to produce a broadband pulse (1.5-3.5 MHz). After the parameters selection for the scan of the sample, the frequency dependent signal loss is computed in the frequency domain using the insertion loss method that will be explain in detail in section 3.2.2. The transmitter is also used in a pulse-echo mode allowing measurement of reflections from the front and back of the tissue sample. The of the transmitted pulses is then used to calculate both thickness and speed of sound.

3.2.2 Method for determining Attenuation Coefficient and Speed of Sound

3.2.2.1 Attenuation Coefficient

The ultrasound attenuation was determined using a fixed path Finite-Amplitude Insertion-Substitution (FAIS) method.[37] As mentioned in section2.3.1, this

CHAPTER 3. MATERIALS AND METHODS FOR ACOUSTIC CHARACTERISATION IN BIOLOGICAL TISSUES

method avoids problems due to diffraction losses.

Considering the scheme in Figure 2.2, this method employs two transducers facing each other, one as a transmitter and the other as a receiver. The attenuation coefficient of a sample is calculated by comparing the received signal through the tissue to that transmitted through the reference water path.

The attenuation coefficient $\alpha(f)$ at a frequency f in units of $dBcm^{-1}$ is therefore:

$$\alpha(f) = \frac{20}{\delta x} (\log_{10} V'(f) - \log_{10} V(f)) \quad (3.1)$$

where δx is the sample thickness, $V'(f)$ is the voltage spectra of the received signal through the sample and $V(f)$ is that of water.

Equation 3.1 assumes that the attenuation coefficient in water is negligible, ignores losses due to transmission at the window interfaces and it also neglects forward scattering.

3.2.2.2 Speed of Sound

Using the system illustrated in Figure 2.2, the average speed of sound over the total tissue path traversed by the sound beam can be calculated with the following equation:

$$c_S = \frac{2X_S}{(t_B - t_F)} \quad (3.2)$$

where

$$X_S = c_W \left[\frac{(t_B - t_F)}{2 - (t_T - t_R)} \right] \quad (3.3)$$

and X_S is the sample thickness; t_B and t_F are the pulse-echo times from the back and front windows of the sample holder, respectively; t_T is the transmit-receive time for the signal to propagate through the sample, t_R is the reference transmit-receive time for the signal to propagate through water in the absence of the sample and c_W is the speed of sound in water. The speed of sound in water is estimated by the use of the thermocouple in the water tank. The measurement of temperature allows us to calculate the speed of sound of the water according to the polynomial equation by [55]:

$$c = 1.402385 \times 10^3 + 5.038813 \times 10^{-2}T^2 + 3.287156 \times 10^{-4}T^4 - 1.398845 \times 10^{-6}T^4 + 2.787860 \times 10^{-9}T^5 \quad (3.4)$$

Figures 3.5 and 3.6 illustrate a typical pulse-echo pulses and transmission pulses including the time shift due to change in sound speed in the sample compared to water.

CHAPTER 3. MATERIALS AND METHODS FOR ACOUSTIC CHARACTERISATION IN BIOLOGICAL TISSUES

The accuracy of the measurements in soft tissues are limited to the accuracy of the reference measurements and the determination of the sample thickness.

3.2.3 Data analysis

The digitise reference (water only path) and attenuated (sample inserted) pulses are computed using the Fast Fourier transform to obtain a frequency dependent signal loss (see Figure 3.5). The speed of sound and the thickness of the sample are calculated.

The attenuation coefficient is derived by calculating the total attenuation and dividing by the estimate thickness (as in Equation 3.1).

A power law fit ($\mu = \alpha f^n$, α and n , are constants and f is the frequency) and a linear fit ($\mu = bf + c$, where b and c are constants) are applied to the frequency dependent attenuation coefficient data (Figure 3.6).

After the calculations, the program plots the resulting parameters in a form of coloured maps, where each coloured square represents a particular position within the sample. An example of the maps that can be obtained are shown in Figures 3.7, 3.8 and 3.9. These measurements were done with a castor oil sample (normally used as a reference liquid), with a grid size of 20x20 mm and a step size of 2x2 mm, at a temperature of 23°C.

The final results are inserted automatically into the yellow boxes represented in Figure 3.3 so that: a) the user can see them; and b) they can then be used for B/A measurement and c) allow editing in the case of errors. The program also saves .mat and excel files of the collected data to later be processed by the user.

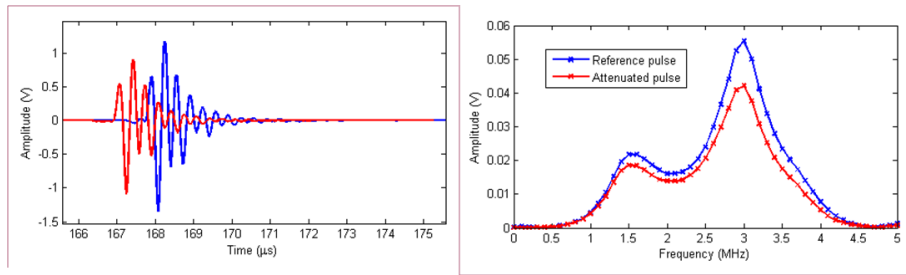


Figure 3.5: Left: Digitise reference (blue) and attenuated (red) pulse; Right: Fourier transform of the pulses

CHAPTER 3. MATERIALS AND METHODS FOR ACOUSTIC CHARACTERISATION IN BIOLOGICAL TISSUES

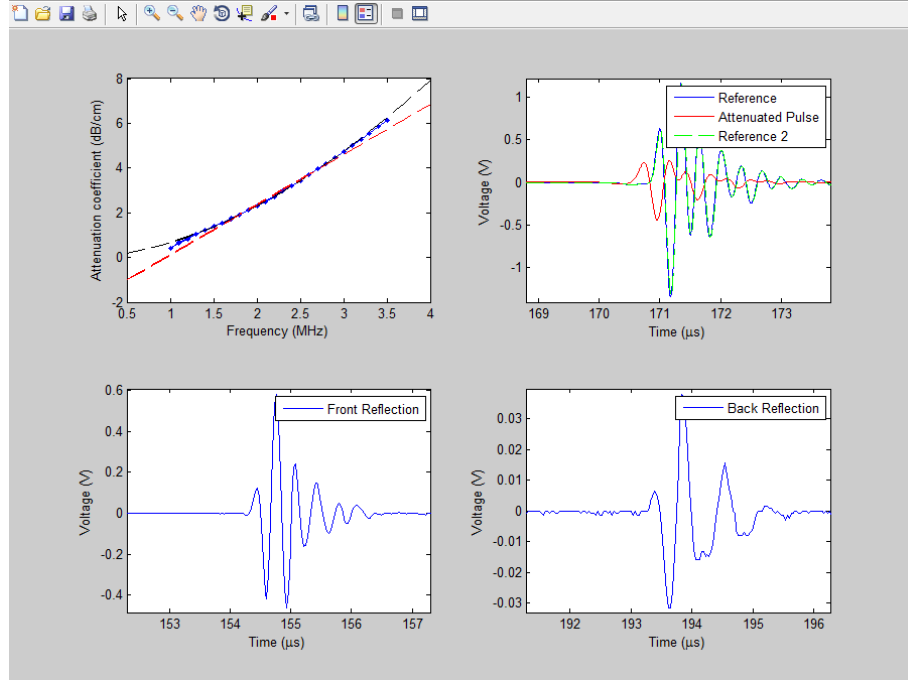


Figure 3.6: Example of a the typical plots obtained with the code for the attenuation and speed of sound measurements. Top: Left - Attenuation coefficient vs. frequency where $\mu = \alpha f^n$; Right - Reference pulses and attenuated pulse. Bottom: Left - Front reflection pulse; Right - Back reflection pulse.

3.2.3.1 Post-processing

It is important to identify which measurements can be rely and which ones have to be discard for several reasons, such as edge effects, presence of blood vessels in the sample, failed waveform digitisation, unrealistically high/low attenuation, hardware-related failure, etc.

For example, observing Figure 3.10, it is possible to distinguish the shape of the sample. The darker blue pixels correspond to the coupling medium, in this case water and we can also detect at the bottom of the maps higher values of attenuation that might be due to the reasons denoted previously. By processing the data as it is, we would obtain erratic attenuation coefficients values regarding the tissue itself. By removing the outliers, the final prediction for the coefficient will be closer to the reality.

For that purpose, it was used a program with an interactive feature that allows the user to select which measurements to remove, leaving only reliable data from which it can be derived the final statistical analysis.

The program works by plotting the total attenuation maps at the selected

CHAPTER 3. MATERIALS AND METHODS FOR ACOUSTIC CHARACTERISATION IN BIOLOGICAL TISSUES

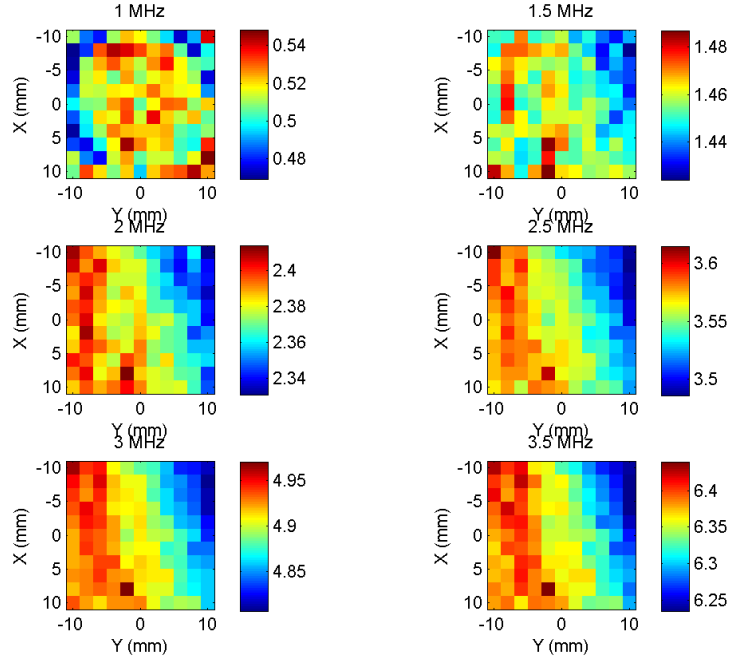


Figure 3.7: Attenuation Coefficients maps at selected frequencies. Colour scale - dB/cm; Sample - castor oil; Grid Size - 20x20 mm; Step Size - 2x2 mm

frequencies one by one in turn, followed by the thickness and then the speed of sound. The idea is to eliminate the pixels one by one that the user considers unreliable and remove from the final computation. Once it has finished, it saves an updated version of the *.mat* file and the Excel file.

CHAPTER 3. MATERIALS AND METHODS FOR ACOUSTIC CHARACTERISATION IN BIOLOGICAL TISSUES

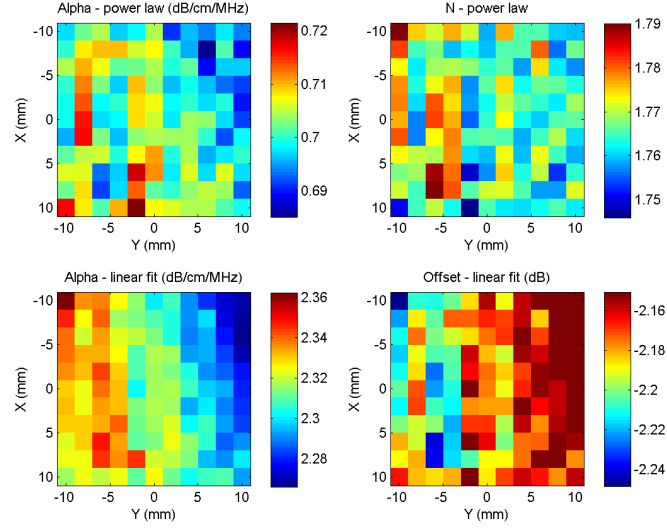


Figure 3.8: Frequency dependency fit parameters maps. Sample - castor oil;
Grid Size - 20x20 mm; Step Size - 2x2 mm

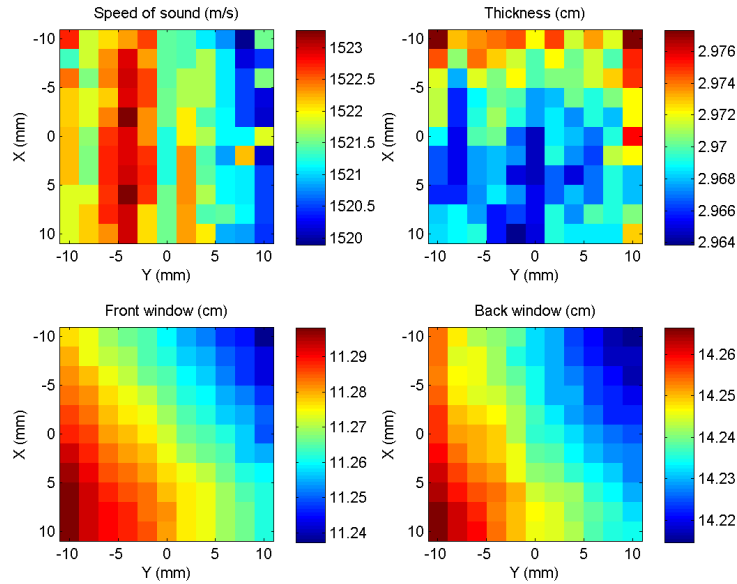


Figure 3.9: Top: Thickness and Speed of Sound maps; Bottom: Front and Back window reflections maps. Sample - castor oil; Grid Size - 20x20 mm; Step Size - 2x2 mm

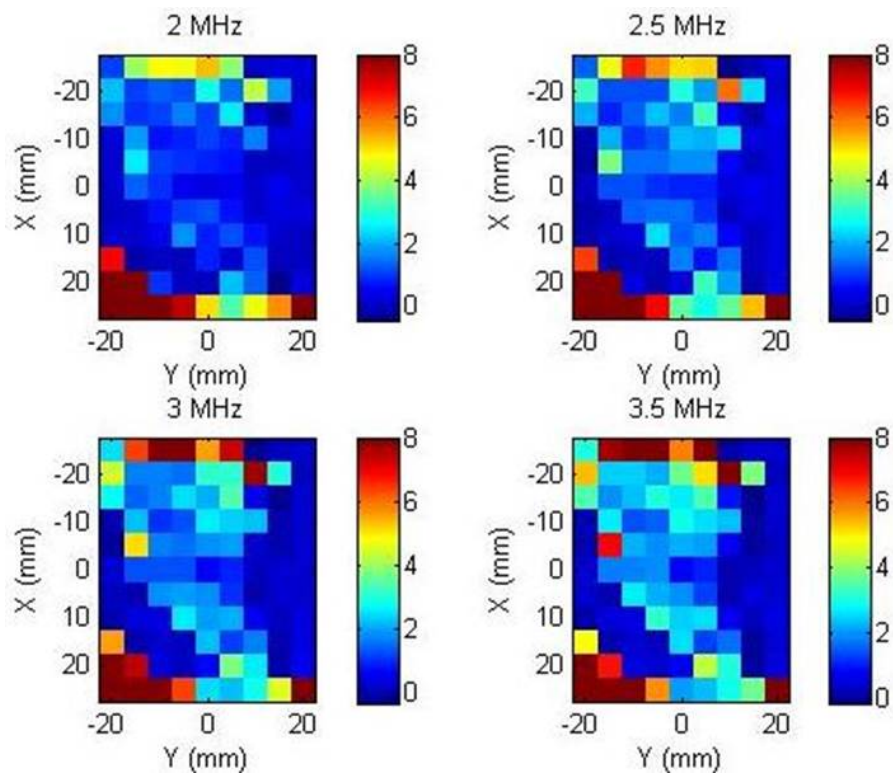


Figure 3.10: Attenuation coefficient maps at selected frequencies. Colour scale - dB/cm; Grid Size - 50x40 mm; Step Size - 4.5x4.5 mm; Sample - human liver tissue

3.3 Non-linearity coefficient

One of the aims of this project is to determine liver tissue non-linearity coefficients (B/A) to improve the accuracy of prediction of acoustic fields for HIFU treatment. This section describes the method used for characterisation of the non-linear properties of the tissue.

3.3.1 Experimental Arrangement

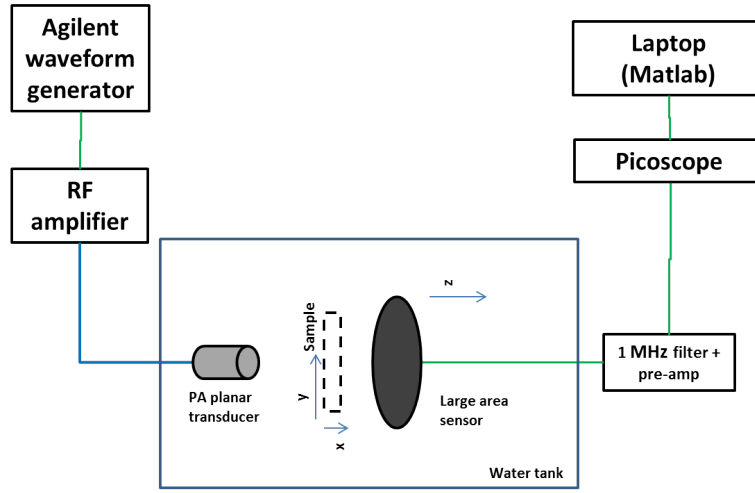


Figure 3.11: Experimental Arrangement for the B/A measurements

The experimental arrangement is shown in Figure 3.11. An arbitrary waveform generator (Agilent 33220A, Agilent Technologies, Inc., Santa Clara, Calif., USA) was used to create a 20 sin cycles 1 MHz transmitted pulse. The pulses were amplified using a RF power amplifier and then used to excite a 1 MHz, 25 mm diameter planar circular transducer (PA347, Precision Acoustics, UK). Ultrasound signals were detected using a membrane hydrophone with a 30 mm active-element diameter (Precision Acoustics, UK) to be most sensitive at 2 MHz. The use of such large area receiver filters out diffraction effects and allows us to assume a plane wave propagation model giving some confidence in the use of the method used that will be describe later.

The measurement is done so that there should be 2 cm between the transducer and the front surface of the sample, and there should be 2 cm between the back surface of the sample and the membrane hydrophone at the first detector (Z) position. The detector Z position steps increase by 10 mm.

Following detection, the signal was passed through an electronic 1 MHz band stop filter to reduce the fundamental, thus maximising the signal of the pressure of the second harmonic. The signal was digitised using a picoscope and sent to a PC to be processed and analysed via a Matlab interface.

3.3.2 Method for determining B/A coefficient

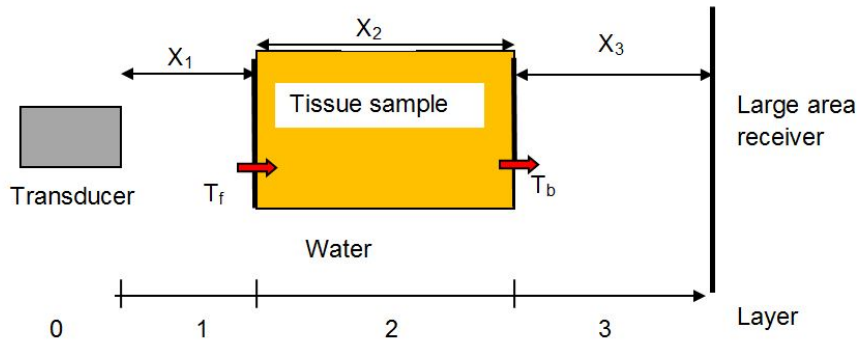


Figure 3.12: Diagram of the typical experimental set up showing the 3 propagation layers, propagation distances (X), transmission coefficients at the front and back windows (T_f and T_b respectively)

In section 2.3.3 were described the available methods for the determination of the B/A coefficient. The method for measuring B/A coefficient of the samples was adapted from [30]. The method involves the measurement of the amplitude of the second harmonic following transmission with and without degassed water displaced by the sample.

The development of the second harmonic in a homogeneous medium due to non-linear propagation and assuming plane wave condition can be estimated using the following expression: [30]

$$P_2(x, P_0) = \frac{\omega(B/A + 2)P_0^2}{4\rho c^3} x e^{-(\alpha_1 + \alpha_2/2)x} \quad (3.5)$$

where ρ is the density, c is the speed of sound, ω is the frequency in rad/s , x is the propagation distance and P_0 is the initial pressure amplitude at the fundamental. Equation 3.5 is considered valid as long as the pressure amplitude of the second harmonic is maintained small relative to the fundamental ($< 1\%$) and $\alpha_2 - 2\alpha_1$ is small ($<< 1$). [30]

The second harmonic that reaches the sensor is the result of non-linear propagation, attenuation and transmission as the wave propagates through

CHAPTER 3. MATERIALS AND METHODS FOR ACOUSTIC CHARACTERISATION IN BIOLOGICAL TISSUES

the 3 different layers shown in Figure 3.12. one way to simplify the problem is by considering the overall pressure amplitude at the second harmonic to be equal to the sum of 4 components:

- $P_{2,0}$ second harmonic generated by the transducer
- $P_{2,1}$ second harmonic developed in layer 1
- $P_{2,2}$ second harmonic developed in layer 2
- $P_{2,3}$ second harmonic developed in layer 3

Function F describes the non-linear development of the second harmonic in the medium m :

$$F(x, P_0)_m = \frac{\omega(B/A_m + 2)P_0^2}{4\rho_m c_m^3} x e^{-(\alpha_{m1} + \alpha_{m2}/2)x} \quad (3.6)$$

We can obtain function F' that is independent of the source pressure amplitude:

$$F'(x)_m = \frac{F(x, P_0)_m}{P_0^2} \quad (3.7)$$

Following the scheme in Figure 3.12, if layers 1 and 3 are the reference medium and layer 2 in denoted by m , the amplitude at the fundamental at the end of each layer can be described as follow:

$$P_{1,0} = P_{1,0} \quad (3.8)$$

$$P_{1,1} = P_{1,0} e^{-\alpha_{w1}x_1} T_{fm1} \quad (3.9)$$

$$P_{1,2} = P_{1,0} e^{-(\alpha_{w1}x_1 + \alpha_{m1}x_2)} T_{fm1} T_{bm1} \quad (3.10)$$

Where $P_{1,0}$ is the pressure amplitude at the fundamental generated by the transducer, $P_{1,1}$ is the pressure amplitude at the fundamental at the end of layer 1, $P_{1,2}$ is the pressure amplitude at the fundamental at the end of layer 2. α_{w1} and α_{m1} correspond to the attenuation coefficients in water and in the medium m at 1 MHz, respectively. T_{fm1} and T_{bm1} represent the transmission coefficients at the front and back window at 1 MHz, respectively.

The second harmonic components measured at the sensor can be derived as:

$$P_{2,0} = P_{2,0} e^{-(\alpha_{w2}x_1 + \alpha_{m2}x_2 + \alpha_{w2}x_3)} T_{fm2} T_{bm2} \quad (3.11)$$

$$P_{2,1} = F'(x_1)_w P_{1,0}^2 e^{-(\alpha_{m2}x_2 + \alpha_{w2}x_3)} T_{fm2} T_{bm2} \quad (3.12)$$

$$P_{2,2} = F'(x_2)_m P_{1,1}^2 e^{-(\alpha_{w2}x_3)} T_{bm2} \quad (3.13)$$

CHAPTER 3. MATERIALS AND METHODS FOR ACOUSTIC CHARACTERISATION IN BIOLOGICAL TISSUES

$$P_{2,3} = F'(x_3)_w P_{1,2}^2 \quad (3.14)$$

Where $P_{2,0}$ corresponds to the pressure amplitude of the second harmonic generated by the transducer, $P_{2,1}$, $P_{2,2}$ and $P_{2,3}$ correspond to the pressure amplitude of the second harmonic in each layer. α_{w2} and α_{m2} correspond to the attenuation coefficients in water and in the medium m at 2 MHz, respectively.

For the case of 3 layers of water (no tissue inserted), the total second harmonic measured at the sensor is therefore:

$$P_{2w} = P_{2,0}g_{w0} + P_{1,0}^2(F'(x_1)_wg_{w1} + F'(x_2)_wg_{w2} + F'(x_3)_wg_{w3}) \quad (3.15)$$

where

$$g_{w0} = e^{-(\alpha_{w2}(x_1+x_2+x_3))} T_{fm2} T_{bm2} \quad (3.16)$$

$$g_{w1} = e^{-(\alpha_{w2}(x_2+x_3))} T_{fm2} T_{bm2} \quad (3.17)$$

$$g_{w2} = e^{(-2\alpha_{w1}x_1)} T_{fw1}^2 e^{-\alpha_{w2}x_3} T_{bm2} \quad (3.18)$$

$$g_{w3} = e^{(-2\alpha_{w1}(x_1+x_2))} (T_{fw1} T_{bw1})^2 \quad (3.19)$$

In the case of a propagation through a tissue sample (corresponding to layer 2) the following equation is obtained:

$$P_{2t} = P_{2,0}g_{t0} + P_{1,0}^2(F'(x_1)_wg_{t1} + F'(x_2)_tg_{t2} + F'(x_3)_wg_{t3}) \quad (3.20)$$

where

$$g_{t0} = e^{-(\alpha_{w2}(x_1+x_3)-\alpha_{t2}x_2)} T_{ft2} T_{bt2} \quad (3.21)$$

$$g_{t1} = e^{(-\alpha_{t2}x_2-\alpha_{w2}x_3)} T_{ft2} T_{bt2} \quad (3.22)$$

$$g_{t2} = e^{(-2\alpha_{w1}x_1)} T_{ft1}^2 e^{(-\alpha_{w2}x_3)} T_{bt2} \quad (3.23)$$

$$g_{t3} = e^{(-2\alpha_{w1}x_1-1\alpha_{t1}x_2)} (T_{ft1} T_{bt1})^2 \quad (3.24)$$

The ratio of the measured second harmonic can thus be expressed by the following equation after division by $P_{1,0}^2$:

$$r = \frac{P_{2t}}{P_{2w}} = \frac{\frac{P_{2,0}}{P_{1,0}^2}g_{t0} + (F'(x_1)_wg_{t1} + F'(x_2)_tg_{t2} + F'(x_3)_wg_{t3})}{\frac{P_{2,0}}{P_{1,0}^2}g_{w0} + (F'(x_1)_wg_{w1} + F'(x_2)_wg_{w2} + F'(x_3)_wg_{w3})} \quad (3.25)$$

The B/A parameter for the tissue sample can be derived by re-arranging equation 3.25:

$$F'(x_2)_t = \frac{r \left(\frac{P_{2,0}}{P_{1,0}^2} + (F'(x_1)_wg_{w1} + F'(x_2)_wg_{w2} + F'(x_3)_wg_{w3}) \right)}{\frac{g_{t2}}{\frac{P_{2,0}}{P_{1,0}^2} (F'(x_1)_wg_{t1} + F'(x_3)_wg_{t3})}} \quad (3.26)$$

CHAPTER 3. MATERIALS AND METHODS FOR ACOUSTIC CHARACTERISATION IN BIOLOGICAL TISSUES

It is possible to assume that the term $P_{2,0}$ that represents the second harmonic generated from the source negligible in certain circumstances. Assuming any second harmonic generated at the transducer is linear with drive amplitude, the effect of this term on the estimate of F' will be reduced as the drive level is increased (as it is divided by the square of $P_{1,0}$). So, maintaining a high drive level it is possible to minimise the effect of any second harmonic generated by the transducer. In this case, equation 3.26 can be simplified to:

$$F'(x_2)_t = \frac{F'(x_1)_w(rg_{w1} - g_{t1}) + F'(x_3)_w(rg_{w3} - g_{t3}) + F'(x_2)_wrg_{w2}}{g_{t2}} \quad (3.27)$$

The drive level should not be so high however that the magnitude of the second harmonic that is generated in the media becomes too large as this will begin to reduce the magnitude of the fundamental which in the derivation above is only affected by attenuation and transmission losses and not by the effect of harmonic pumping which is considered to remain negligible.

Finally, the B/A coefficient of the tissue sample is given by:

$$\left(\frac{B}{A}\right)_t = \frac{4F'(x_2)_t\rho_t c_t^3}{\omega x_2 e^{-(\alpha_{t1} + \alpha_{t2})x_2}} - 2 \quad (3.28)$$

3.3.3 Data analysis

The data were transferred from the oscilloscope to a Laptop via a GPIB port. A Matlab interface was used to window the 5 cycles of interest automatically, and then to Fourier transform the recorded signal in order to provide the amplitude of the frequency spectrum at the second harmonic.

As it happens with the attenuation coefficient maps, the B/A maps obtained require the removal of pixels that are consider unrealistic. As seen in Equation 3.28, the non-linearity coefficient is dependent of the values of the attenuation at the fundamental and at the second harmonic. If an outlier removal was carried out for the attenuation and speed of sound maps, it is also necessary to correct these constants before pursuing with the B/A measurement scan. This can be done manually by changing the values marked in yellow at the Matlab interface (see Figure 3.3).

The process of removing the outliers is the same for the attenuation and speed of sound maps.

CHAPTER 3. MATERIALS AND METHODS FOR ACOUSTIC CHARACTERISATION IN BIOLOGICAL TISSUES

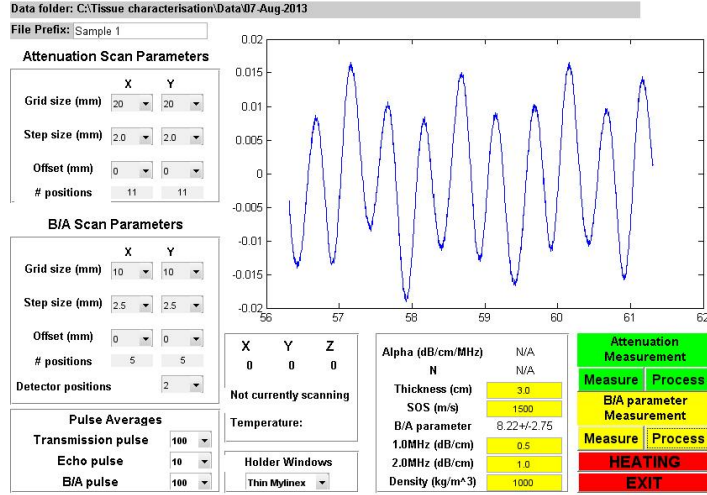


Figure 3.13: An example of the software during B/A measurement with a typical waveform.

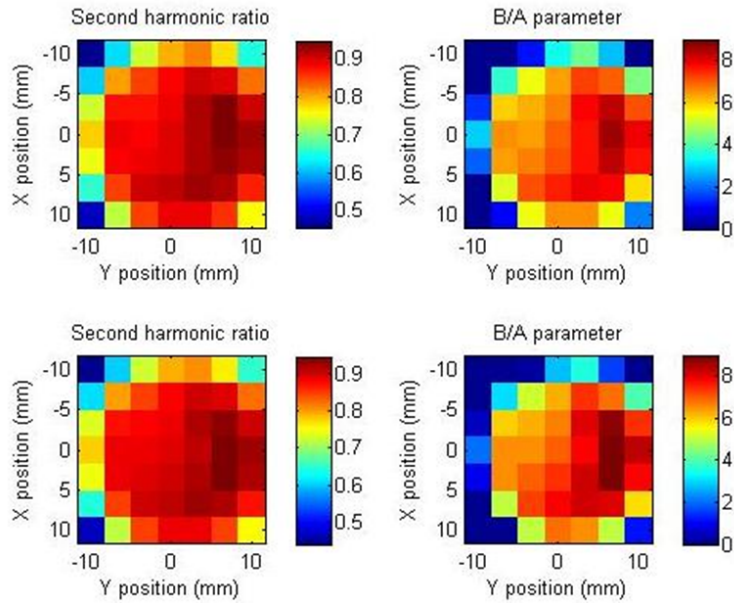


Figure 3.14: Left: Second Harmonic Ratio maps ($\frac{P_{2t}}{P_{2w}}$); Right: B/A parameter maps. The acquisition was done for 2 sensor positions.

3.4 Experimental Protocols

3.4.1 Animal experiments

The measurements of the attenuation coefficient, speed of sound and B/A coefficient were determined for fresh bovine and porcine livers.

Each sample was cut into a cylindrical or square shape with approx. 2 cm in thickness using a cutter and mounted in the holders under degassed water (Figure 3.15). It was important to make sure that the samples surfaces were smooth and that there were parallelism between the sides.

A total of three fresh ex-vivo livers were analysed. For the bovine liver, three sets of measurements were made in samples obtained from different locations of the lobe. For the two porcine livers, a total of three samples were mounted and analysed. For both cases each measurements were done in the following way:

1. Maintained at room temperature (22 °C);
2. Water bath heated to 37 °C;
3. Water bath heated to 44 °C (only for the porcine samples).

Table 3.1: List of the measurements done for each animal ex-vivo sample.

Tissue	Sample no.	Measurements			Temperature (°C)	
		Attenuation	Speed of sound	B/A	20	38
Bovine	1	✓	✓	✓	✓	✓
	2	✓	✓	✓	✓	✓
Porcine #1	1	✓	✓	-	✓	✓
Porcine #2	2	✓	✓	✓	-	✓
	3	✓	✓	✓	-	✓

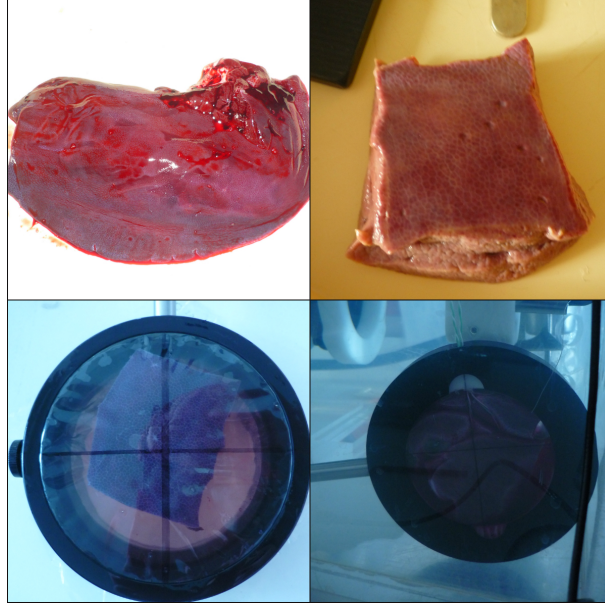


Figure 3.15: Example of an ex-vivo animal sample preparation. Top Left: Portion of a liver; Top Right: Sample cut in a square shape with parallel sides; Bottom Left: Sample mounted in the holder; Bottom Right: Sample in the water tank;

3.4.2 Human tissue experiments

The specimens of human liver were obtained from liver resection patients at the Royal Free Hospital. The time between the excision of the organ and the experiments were never more than one hour. Six specimens of human liver of varying pathology were analysed. The detailed characteristics of the samples types and their measurements are shown in Table 3.2.

The experimental protocol used was the following:

- water bath heated to 38°C;
- samples were mounted in the holders (within saline solution or degassed water) and photographed;
- samples were placed in the water tank and scanned at 38°C;
- one specimen (liver number 3) was scanned also at 44°C and 50°C.

For each specimen sample measurements of attenuation and speed of sound were conducted. Due to problems related with the thickness of the samples available, it was only possible to obtain B/A coefficient values for

CHAPTER 3. MATERIALS AND METHODS FOR ACOUSTIC CHARACTERISATION IN BIOLOGICAL TISSUES

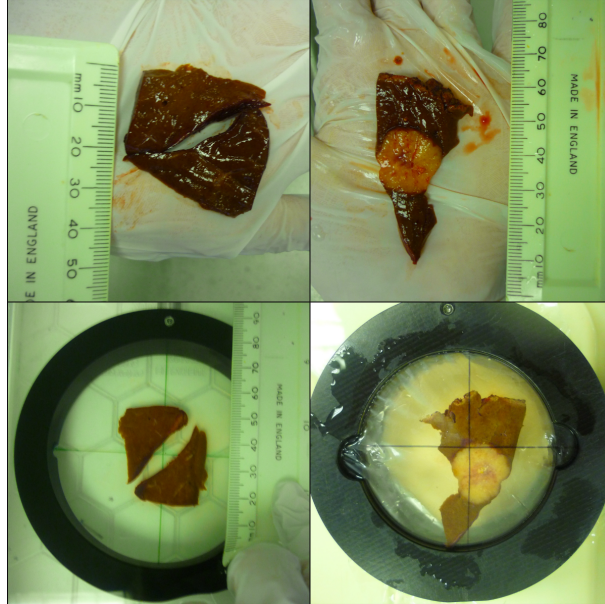


Figure 3.16: Example of an human liver sample preparation. Top Left: Normal liver tissue sample; Top Right: Mixed (normal + tumour) liver tissue sample; Bottom Left and Right: Samples mounted in the holders.

two samples (as indicated in Table 3.2). A total of three tissue types were studied: healthy/normal, tumorous and cirrhotic.

Table 3.2: List of the measurements done in each specimen of human liver, specifying scans conditions

Liver no.	Tissue type	Measurements			Temperature (°C)		No. of scans
		Attenuation	Speed of sound	B/A	38	50	
1	Fatty	✓	✓	✓	✓	-	1
	Fatty	✓	✓	✓	✓	-	1
	Tumour	✓	✓	-	✓	-	1
2	Mixed (tumour+normal)	✓	✓	-	✓	-	5
	Normal	✓	✓	-	✓	-	3
3	Tumour	✓	✓	-	✓	✓	8
4	Normal	✓	✓	✓	✓	-	2
	Mixed (tumour+normal)	✓	✓	-	✓	-	2
5	Cirrhotic	✓	✓	✓	✓	-	2
	Tumour	✓	✓	✓	✓	-	2
6	Normal	✓	✓	✓	✓	-	3
	Tumour	✓	✓	✓	✓	-	1

Chapter 4

Acoustic Properties of Human Liver Tissue

4.1 Validation Experiments

In view of the large number of possible sources of error in measuring an attenuation coefficient, and the difficulty of estimating many of them, it is advisable to check any new measurement system by performing measurements on standard materials that have known characteristics that are widely agreed upon.

For systems designed to make relative measurements on tissues, a phantom incorporating beam distortion and the appropriate amount of scattering is not yet available. Castor oil forms a suitable homogeneous test material, chosen by many for this purpose because there is good agreement on its ultrasonic attenuation properties, and its ultrasonic speed are of similar magnitudes to those of many soft tissues at room temperature.

4.1.1 Cryogel phantoms

Tissue-mimicking phantoms can help in uncovering potential weaknesses in medical imaging systems. PVA-cryogel is as a tissue-mimicking material with acoustic and shear elasticity properties optimized to best represent those of liver tissue.

This type of cryogel is form by adding polyvinyl alcohol in a water solution which is then solidified through a freeze-thaw process. The number of freeze-thaw cycles affects the properties of the material. Four cryogel samples were used, each sample solidified through different numbers of freeze-thaw cycles.

In Figure 4.1 is plotted the attenuation coefficients in function of the frequency for the four samples analysed. The speed of sound was found

CHAPTER 4. ACOUSTIC PROPERTIES OF HUMAN LIVER TISSUE

to range from 1570.8 to 1573.3 m/s, with mean and standard deviation of 1571 ± 1.07 m/s and the attenuation coefficients were in the range of 0.19-0.33 dB/cm/MHz with mean and standard deviation of 0.24 ± 0.06 dB/cm/MHz.

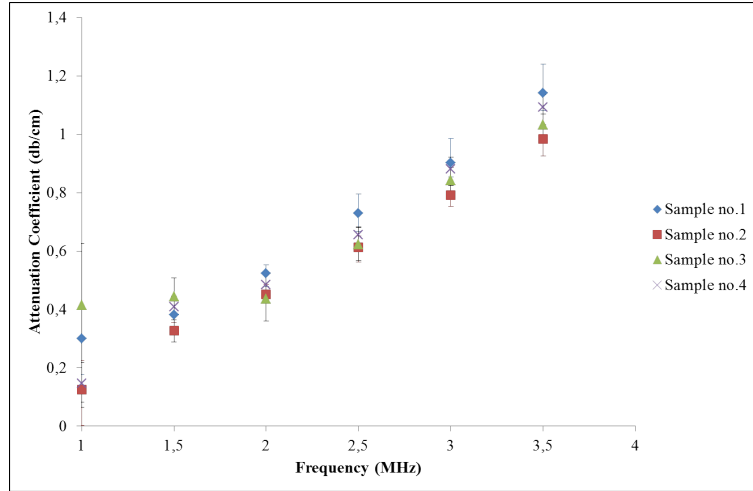


Figure 4.1: Measured attenuation coefficient versus frequency.

Table 4.1: Acoustic properties measured of the reference media: cryogel

Sample no.	α (dB/cm/MHz)		N		Speed of Sound (m/s)		B/A	
	Mean	STD	Mean	STD	Mean	STD	Mean	STD
1	0.224	0.046	1.274	0.151	1570.8	1.30	1.68	4.17
2	0.190	0.021	1.274	0.151	1571.7	0.69	4.73	0.45
3	0.326	0.504	1.291	0.060	1573.3	1.73	5.84	2.09
4	0.240	0.067	1.342	1.275	1571.5	1.27	4.54	0.27

4.1.2 Reference liquids

4.1.2.1 Reference sample: Castor Oil

Castor oil forms a suitable homogeneous test material because there is good agreement on its acoustic properties, and its ultrasonic speed and attenuation are of similar magnitudes to those of many soft tissues. Published speed of sound and attenuation coefficients for castor oil are presented in Table 4.2.

The frequency dependent absorption coefficient for castor oil at 30°C is $5.8f^{1.667}$ neper m^{-1} over the range 400 kHz to 500 MHz (see Dunn et al. 1969) where f is the frequency in MHz.

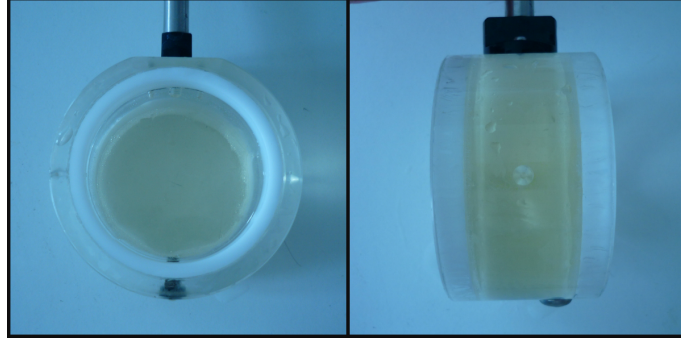


Figure 4.2: Castor oil sample.

Table 4.2: Published Velocity and Attenuation coefficient for Castor Oil. [22]

Temperature (°C)	Speed of sound (m/s)	Attenuation coefficient (neper m^{-1}) at 1MHz
0	1580	26.0
10	1536	16.0
20	1494	9.6
30	1452	5.8
40	1411	3.7

Comparison between values from the holder filled with the standard reference castor oil, measured in our system at 23°C and published data [86] shows agreement, thus establishing the validity of the system.

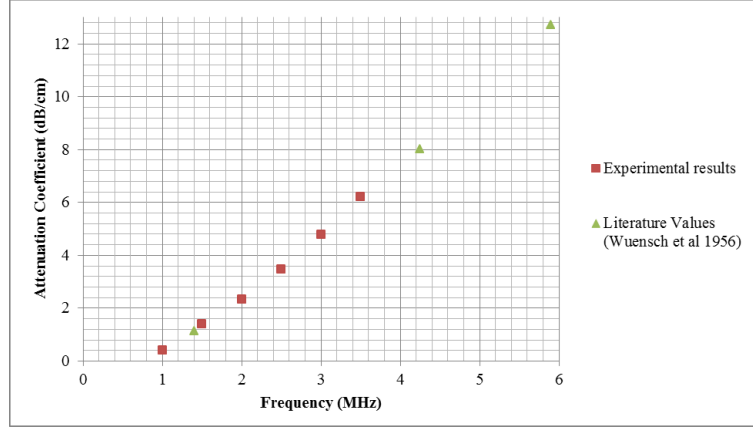


Figure 4.3: Verification of the methods and equipment in the system using Castor Oil and comparison with literature values.

Table 4.3: Acoustic properties of the reference media: degassed water and castor oil.

Material	α (dB/cm/MHz)		N		Speed of Sound (m/s) at 23°C		B/A	
	Mean	STD	Mean	STD	Mean	STD	Mean	STD
Castor Oil	0.686	0.004	1.765	0.006	1519.405	0.21	13.38	0.16
Degassed Water	-	-	-	-	-	-	4.96 5.2 [19]	0.05 0.26 [19]

4.1.3 Characterisation of the second harmonic as a function of distance

In this section we explore the behaviour of the second harmonic as a function of distance. As noted in section 2.2.3, as a monochromatic wave propagates through a medium, it progressively becomes richer in harmonic frequencies of the fundamental.

The acoustic pressure of the second harmonic generated is approximately proportional to the distance travelled by the sound, to the frequency used, and to the pressure of the original signal. [7]

We investigated the generation of the second harmonic through water as the distance between the transmitter and the receiver increases, with the aim of validating the experimental setup used for the measurements of the B/A coefficient and confirm the assumption made by neglecting the term $P_{2,0}$ in Equation 3.26 in section 3.3.2.

CHAPTER 4. ACOUSTIC PROPERTIES OF HUMAN LIVER TISSUE

At each distance z from the transmitter, the pressure of the second harmonic was determined. The transmitter-receiver distance was increased in 5-mm increments. All experimental data were collected in water at room temperature. A 20-cycle sinusoidal pulse was used to excite the transmitter and the signal was detected by the receiver at each of the 26 positions.

The code used to analyse the data is given in Appendix A.1. The processing program reads in the collected data. For each waveform the program segments 5 cycles to determine the second harmonic pressure. The calculation of the time delay for the signal to reach the detector is based on the distance z and the speed of sound in water (at 23°C, 1493 m/s) [54]

$$t = 14 + z \frac{1000}{c} \quad (4.1)$$

where t is the time in microseconds, z is the transmitter-receiver distance and c the speed of sound in water at 23°C.

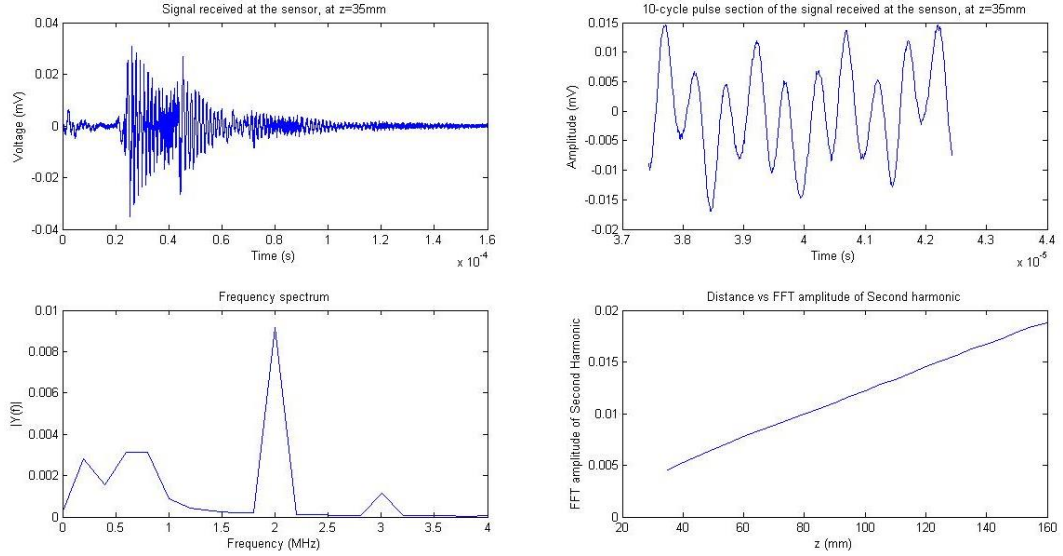


Figure 4.4: Top Left: Signal received at the sensor; Top Right: 10-cycle pulse section of the signal received at the sensor; Bottom Left: Frequency spectrum of the 10-cycle section; Bottom Right: Distance between the transmitter and the receiver versus FFT of the Second Harmonic.

Performing the fast Fourier transform on the segmented signal (Figure 4.4, Top Right), we obtain the frequency spectrum of the signal, where it clearly shows the peak corresponding to the second harmonic (Figure 4.4, Bottom

Left). The magnitude of the second harmonic is then plotted as functions of distance from the transducer (Figure 4.4, Bottom Right).

If we extrapolate the linear trend back to the transducer ($z=0$) we found that it shows that the intercept is low, i.e. there is very little second harmonic at the transducer surface.

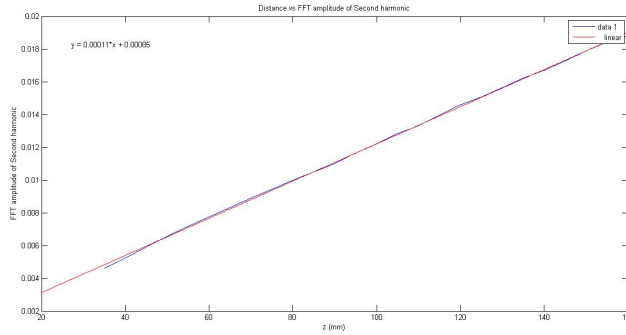


Figure 4.5: Extrapolation of the data to the transducer ($z=0$).

This would be because:

1. there has been no propagation distance for the second harmonic to develop, and
2. there is very little, if any at all, second harmonic emitted by the transducer.

This results show that we can derive the equation 3.28 without having to consider the second harmonic generated at the transmitter and just assume a value of 0.

4.2 Animal ex-vivo experiments

Figures 4.6-4.7 shows examples of the attenuation coefficients in dB/cm as a function of frequency and the speed of sound for bovine liver tissue samples at 20°C and 37°C obtained with the measurement system. Also in the figure is plotted published data from [6]. Standard deviations representing intra-sample variability are shown by vertical bars in figures.

The data obtained are showed in Figures 4.4-4.6 shows the acoustic measurements that have been made in this study.

CHAPTER 4. ACOUSTIC PROPERTIES OF HUMAN LIVER TISSUE

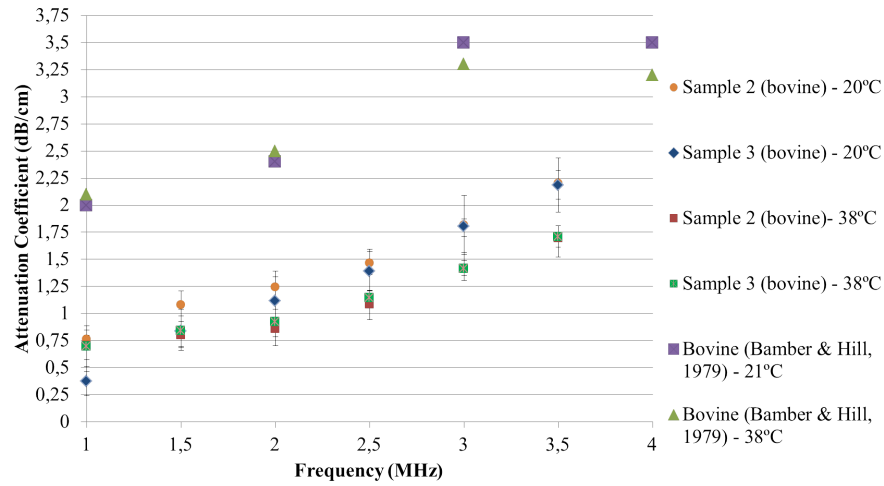


Figure 4.6: Comparison of the attenuation coefficient results for bovine ex-vivo samples obtained with the system and the literature values.

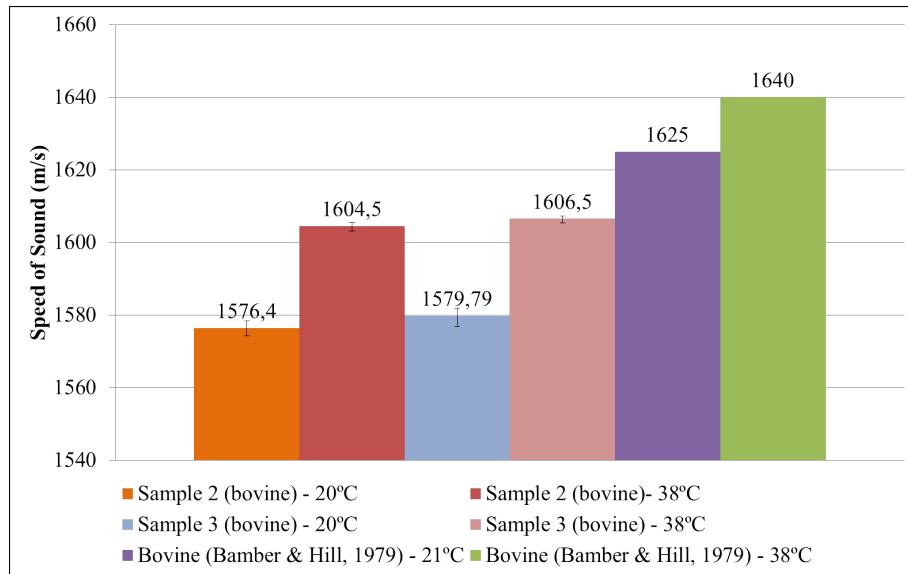


Figure 4.7: Comparison of the speed of sound values for bovine ex-vivo samples obtained with the system and the literature values.

CHAPTER 4. ACOUSTIC PROPERTIES OF HUMAN LIVER TISSUE

Table 4.4: Measured attenuation coefficients in bovine and porcine liver tissue samples; Power fit $\mu = \alpha f^N$

Sample	Temperature °C	α (dB/cm/MHz)		N	
		Mean	STD	Mean	STD
Bovine (sample 1)	20	0.791	0.190	0.732	0.230
	38	0.552	0.218	0.817	0.312
Bovine (sample 2)	20	0.489	0.145	1.129	0.216
	38	0.595	0.238	0.802	0.371
Porcine #1 (sample 1)	20	0.525	0.09	0.965	0.114
	38	1.766	0.93	0.288	0.508
Porcine #2 (sample 2)	20	1.316	0.447	0.550	0.268
	38	0.593	0.312	0.836	0.316
Porcine #2 (sample 3)	20	0.459	0.137	0.912	0.278
	38	0.329	0.06	1.172	0.179

Table 4.5: Measured speed of sound in bovine and porcine liver tissue samples.

Sample	Temperature (°C)	Speed of Sound (m/s)	
		Mean	STD
Bovine (sample 1)	20	1576	2
	38	1604	2
Bovine (sample 2)	20	1579	3
	38	1607	1
Porcine #1 (sample 1)	20	1584	2
	38	1608	2
Porcine #2 (sample 2)	20	1580	2
	38	1601	2
Porcine #2 (sample 3)	20	1578	1
	38	1593	5

CHAPTER 4. ACOUSTIC PROPERTIES OF HUMAN LIVER TISSUE

Table 4.6: Measured B/A coefficients in bovine and porcine liver tissue samples.

Sample	Temperature (°C)	B/A	
		Mean	STD
Bovine (sample 1)	20	5.82	1.29
	38	5.24	0.91
Bovine (sample 2)	20	5.20	0.93
	38	5.90	0.70
Porcine #2 (sample 2)	20	8.96	2.52
	38	5.41	0.59
Porcine #2 (sample 3)	20	6.67	2.03
	38	3.39	1.81

Table 4.7: Published speed of sound and B/A coefficient values.

Tissue	Temperature (°C)	Speed of Sound (m/s)	B/A
Bovine	23	1575-1627 [6]	6.2-8.9 [48]
	37	1597-1639 [6]	-
Porcine	24	1588 \pm 0.5% [31]	-
	37	-	-

4.3 Human Liver Tissue

The results obtain for all the samples are displayed and summarised in Table 4.8.

Table 4.8: Ultrasonic properties measurements in different types of human liver.

	No. livers		α (dB/cm/MHz)	N	Speed of Sound (m/s)	B/A
Healthy	3	range:	0.32 – 0.96	0.84-1.55	1552-1577	-
		mean:	0.59 ± 0.33	1.24 ± 0.37	1571 ± 17	
Tumour	4	range:	0.29-1.55	1.09-1.94	1554-1583	4.57
		mean:	0.68 ± 0.60	1.39 ± 0.60	1569 ± 14	
Cirrhotic	1	mean:	1.20 ± 0.72	0.54 ± 0.49	1568 ± 5	-
Fatty	1	mean:	0.51 ± 0.22	1.03 ± 0.33	1596 ± 2	5.46

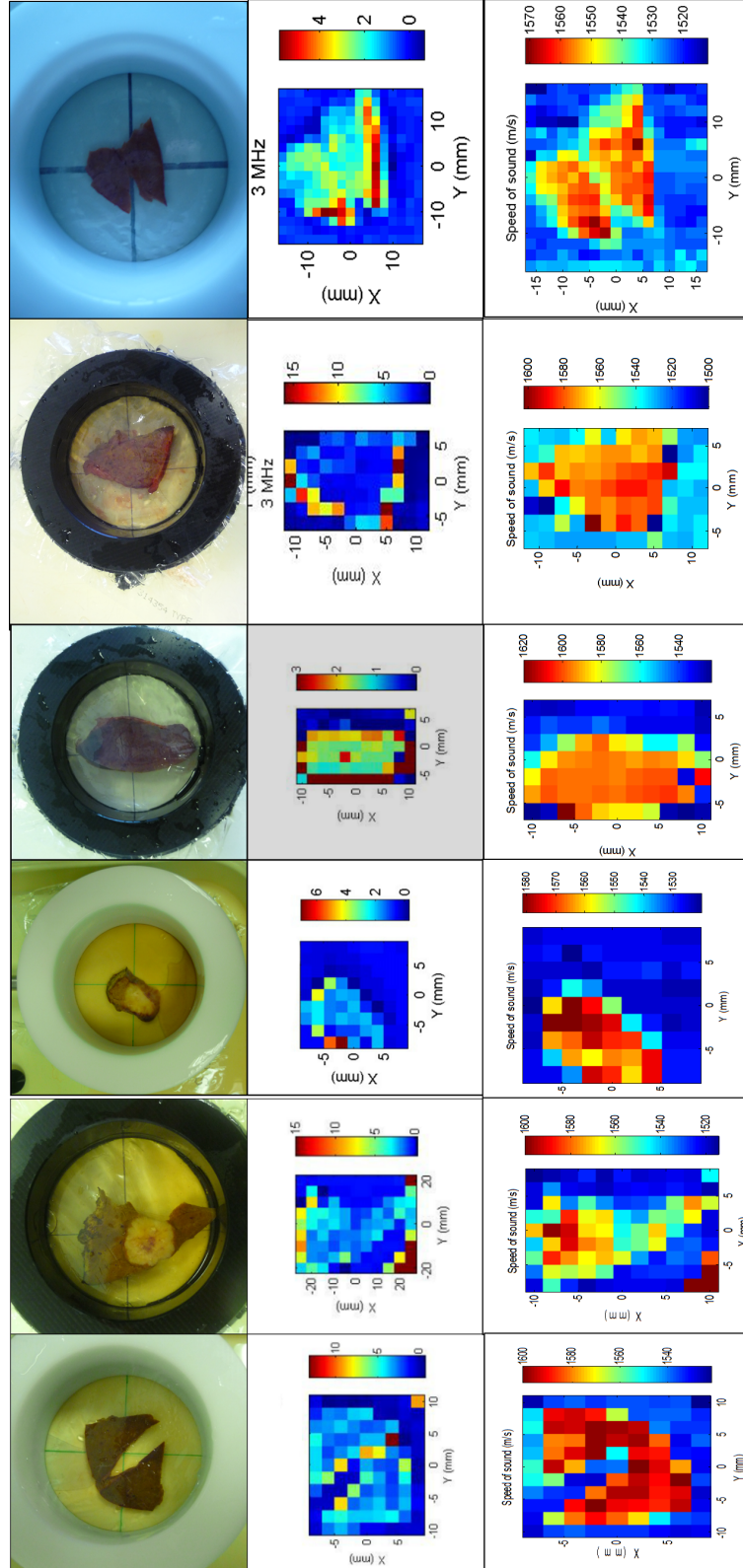


Figure 4.8: Photographs, attenuation at 3 MHz and speed of sound maps of some samples.

4.3.1 Attenuation and Speed of Sound

4.3.1.1 Normal Liver

The observed range of attenuation values in 4 livers was 0.32–0.96 dB/cm/MHz with a mean and standard deviation of 0.59 ± 0.33 dB/cm/MHz. Figure 4.9 shows a comparison between the measured attenuation coefficient in function of the frequency for healthy liver samples and published values. Data points indicate mean values for all data acquired within the scan and error bars represent the total range of values.

For the speed of sound results ranged between 1552 and 1577 m/s with a mean and standard deviation of 1571 ± 17 m/s.

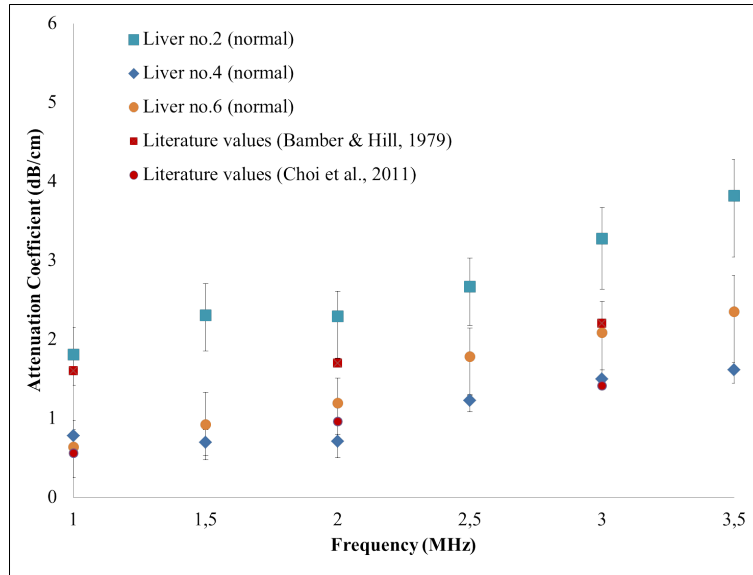


Figure 4.9: Measured Attenuation coefficients for 3 samples in function of frequency.

4.3.1.2 Tumour tissue

The attenuation values measured in tumour samples ranged from 0.29 to 1.55 dB/cm/MHz. The mean and standard deviation of the attenuation in cancerous tissue samples was computed as 0.68 ± 0.60 dB/cm/MHz. In Figure 4.10 is plotted the measured attenuation coefficients in function of the frequency for two livers with both normal and tumorous tissue that were measured separately. Data points indicate mean values for all data acquired within the scan and error bars represent the total range of values.

CHAPTER 4. ACOUSTIC PROPERTIES OF HUMAN LIVER TISSUE

Speed of sound values ranged from 1554 to 1583 with mean value and standard deviation of 1569 ± 14 m/s.

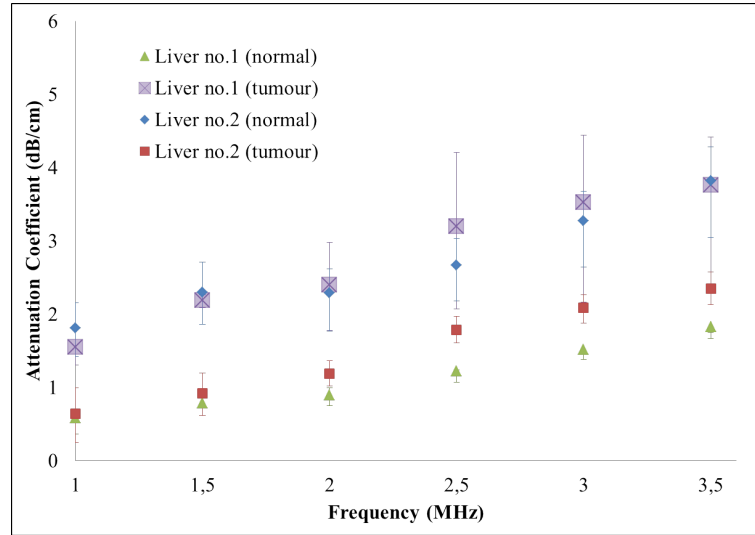


Figure 4.10: Attenuation coefficient in function of frequency: comparison between healthy and tumorous samples.

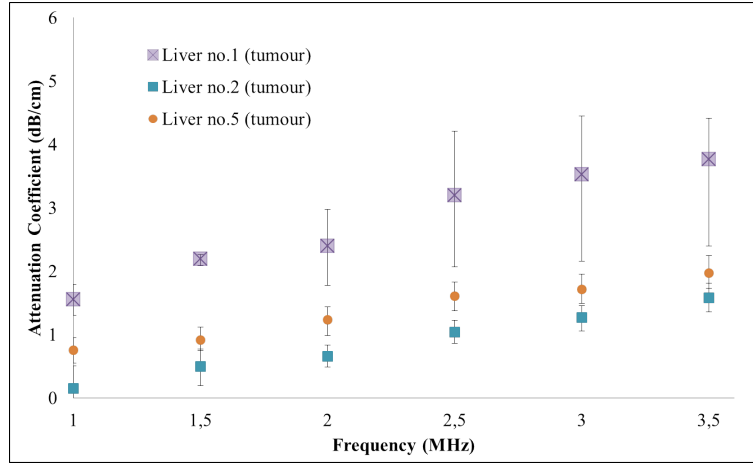


Figure 4.11: Attenuation coefficient in function of frequency:tumour samples.

4.3.1.3 Cirrhotic and Fatty Liver

Only one sample of cirrhotic liver was studied. Results showed an attenuation of 1.20 ± 0.72 dB/cm/MHz and speed of sound of 1568.12 ± 5.29 m/s. The results for the fatty liver sample were the following: attenuation coefficient 0.51 ± 0.22 dB/cm/MHz and speed of sound 1596 ± 2 m/s. Standard deviation values represent the total range of values obtain within the scan.

Table 4.9: Published values for B/A coefficient and Speed of Sound for human liver. [65]

Type	Temperature (°C)	B/A	Speed of Sound (m/s)
Normal	37	6.75 ± 0.14	1592 ± 6
	20	6.31 ± 0.09	1567 ± 6
Fatty (slight)	20	6.87 ± 0.18	1560 ± 5
	37	7.46 ± 0.25	1581 ± 5
Fatty (cirrhosis)	20	6.16	1546
	37	6.07	1562
Tomour	20	-	1555 ± 13
Adenocarcinoma	37	6.58	1584
	20	6.41	1563

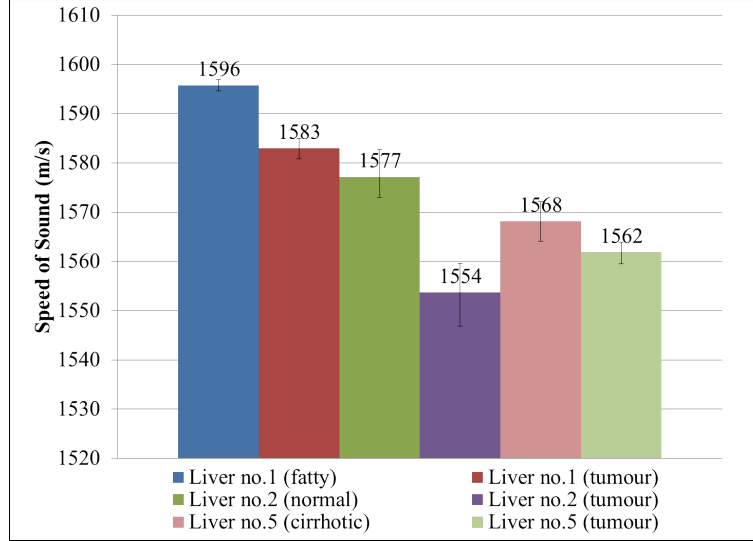


Figure 4.12: Measured Speed of sound values.

4.3.2 B/A coefficient

In Table 4.8 is displayed the average value for the B/A coefficient for fatty tissue (liver no.1) and tumour tissue (liver no.3).

4.3.3 Acoustic properties as a function of temperature

The attenuation coefficient, speed of sound and non-linearity parameter B/A have been determined for one human liver specimen (liver no.3), specifically a tumour sample at two temperatures: 38°C and 50°C. The results for each parameter are displayed below.

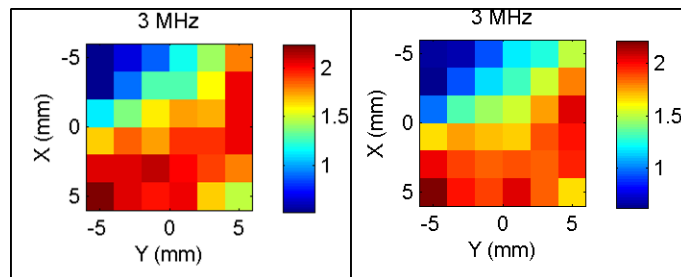


Figure 4.13: Attenuation maps at 3 MHz at 38°C and 50°C (from left to right).

CHAPTER 4. ACOUSTIC PROPERTIES OF HUMAN LIVER TISSUE

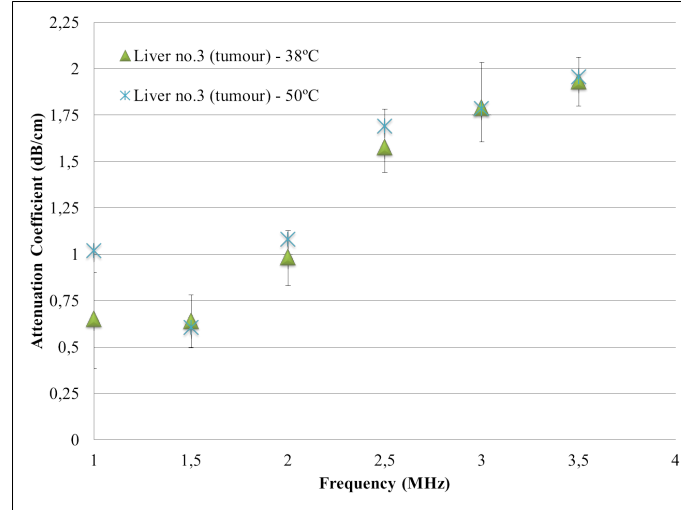


Figure 4.14: Attenuation coefficients in function of frequency at 38°C and 50°C.

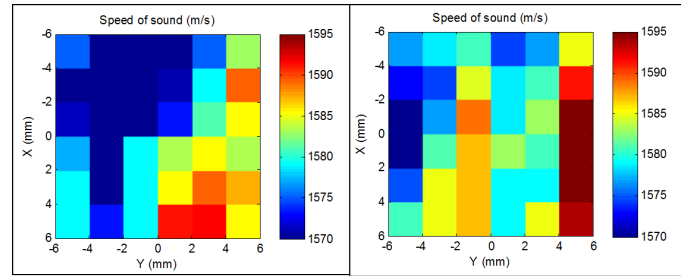


Figure 4.15: Speed of Sound maps at 38°C and 50°C (from left to right).

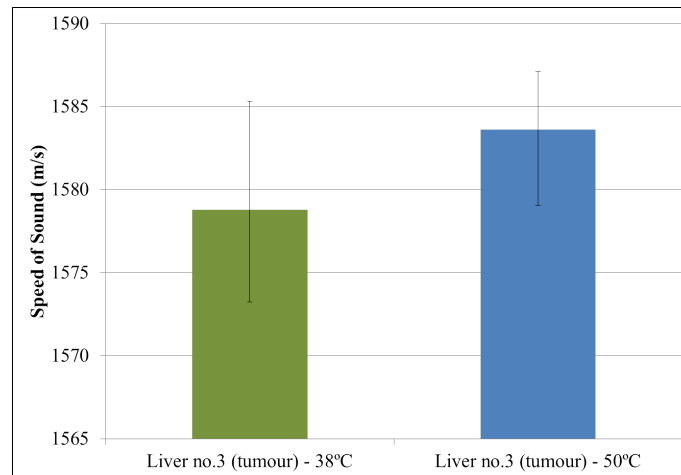


Figure 4.16: Measured Speed of Sound values at 38°C and 50°C.

CHAPTER 4. ACOUSTIC PROPERTIES OF HUMAN LIVER TISSUE

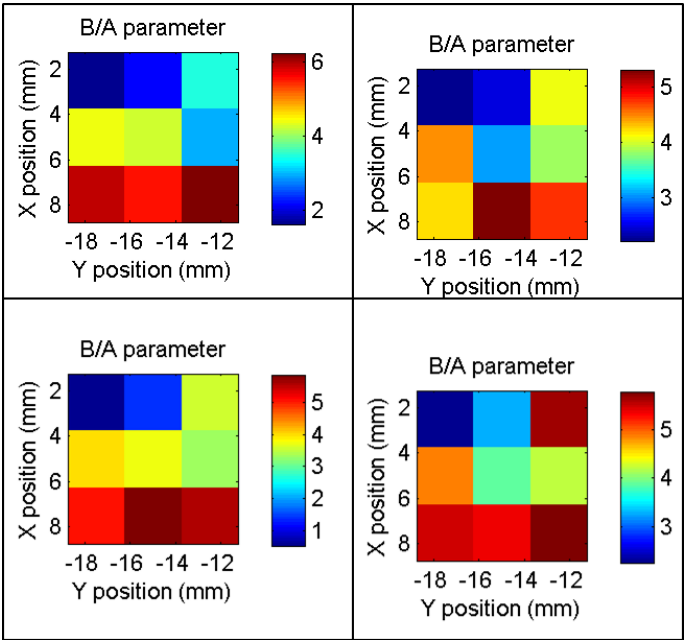


Figure 4.17: B/A coefficient maps at 38°C and 50°C (from left to right).

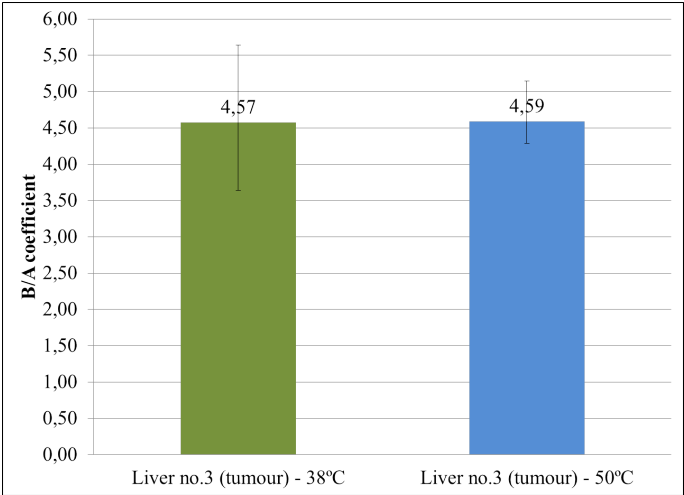


Figure 4.18: Measured B/A coefficient values at 38°C and 50°C.

Chapter 5

Discussion and Conclusions

The acoustic parameters of interest were measured using the all in one tissue characterisation system for a variety of samples: reference samples such as castor oil and degassed water; animal ex-vivo tissues and explant human liver tissue.

5.1 Animal samples

Three fresh ex-vivo liver samples properties were measured using the tissue characterisation system. Looking at the data presented in Figures 4.6 and 4.7, is possible to denote that the values obtained with the system are slightly lower than the one published in literature. Results also show that the attenuation decreases when the temperature increases from 20°C to 37°C. Bamber and Hill observed that for high frequencies, attenuation has a negative dependence on temperature, the value at 20°C being about 21% higher than that at 37°C and as for lower frequencies (around 1-2 MHz, depending with the tissue specimens) they observed the opposite. The same thing is observed with our measurements, particularly for liver no.3. At lower frequencies (in our case 1 MHz), the value at 20°C is lower than that at 37°C.

As for the porcine liver samples, our attenuation coefficients are also lower to the ones published in literature, however it is important to denote that measurements done in different samples from the same liver show no statistical difference (correlation coefficient = 0.998).

Speed of sound values shows an increase with the temperature for both bovine and porcine samples. This was also previously observed which contributes for the validation of this system. However, our results are also lower than the ones published before. This can possibly be explained by the biologically variability in the properties of tissues. Also the fact that we are comparing different techniques and also different methods of preparing or

storing the samples brings the possibility of errors. The lack of explanation of some authors about the tissue conditions (freshly measurements or one day old tissues) also makes this comparison difficult.

There is a lack of data related to the non-linearity coefficient B/A in literature thus making it very difficult to compare our results with previous experiments. However, the experiments made with the reference mediums such as degassed water and castor oil show the ability of our system to measure this parameter.

As a result of the small sample size and no clear pattern observed, it is not statistically possible to draw accurate and statistically significant conclusions at this stage. However, the results show that the system is able to determine the parameters in question. Future studies with a bigger sample size will be required in order to validate the system and also explore thoroughly the relationship between the acoustic properties and temperature variations in the tissue.

5.2 Human liver tissue

The quantification of the attenuation coefficient, speed of sound and the non-linearity coefficient B/A in fresh human liver samples using the "all-in-one" acoustic measurement system in an hospital environment was investigated. A range of different tissue types were studied and comparison with literature values were made. The results obtain for each of the parameters measured are justified below.

The attenuation coefficient data average over all the samples show:

- i Values obtained for normal liver show big variation between samples (Figure 4.9).
- ii Two out of three normal tissue samples show to be within the values observed in literature (Figure 4.9).
- iii large variation within the sample observed by the big error bars (Figures 4.9 and 4.10). One way to tackle this issue in future studies is to use histological data to access homogeneity, structure and composition of the sample in order to make reliable comparisons between samples from different livers that might explain the data variability.
- iv No clear differentiation between tumour and normal tissue (Figure 4.10).

The speed of sound data show:

CHAPTER 5. DISCUSSION AND CONCLUSIONS

- i From all the tissue types, fatty liver presents the higher speed of sound value. This goes against previous studies [4].
- ii Tumour samples present lower speed of sound when compared with normal tissue samples from the same liver. This shows agreement with previous observations [4].

The overall results from the human tissue samples present big error bars, making it unreliable to make accurate conclusions regarding the measurements and the system performance. This issues come down mainly due to the nature of the samples. The main difficulties/shortcomings are detailed bellow:

1. No control over the preparation and cutting of the samples. The samples were cut and given to us by the surgeon in the OR. The reason for such thin samples was because most of the specimen was required for other tests (pathology for example).
2. Thickness subject to potential spatial variation due to the slab cutting process
3. Acoustic measurements (especially B/A coefficient) are highly dependent of the sample thickness
4. FAIS method requires that the samples have parallel-sides. The transmitted signal amplitude depends on the parallelism of the sample sides, which is difficult to achieve accurately when cutting the tissue
5. Errors in determination of speed of sound: accuracy of the reference measurements (water) and determination of the sample thickness

In regards of the B/A experimental set-up, there are some important critics and improvements to tackle:

- i Its basis is the measurement of the amount of the second harmonic generated in the sample. A 20 cycle pulse at 1 MHZ has an equivalent pulse length of 30 mm. In order to ensure that the reflected pulse at the sample front face (and subsequent reflection at the transmitter) does not interfere with the straight-through transmitted pulse the sample has to have a minimum thickness of 15 mm. This was not possible to ensure in our samples due to conflicts beyond our control.
- ii The sample is placed at 2 cm from the transmitter (the minimum separation between transmitter and sample front face has to be at least half

the pulse length). By placing the sample at this distance we are basically placing it in the near field of the transmitter. This contributes for a bad spatial resolution in the B/A maps. A way to overcome this problem is to place the sample in the far field, however this would be limited by the beamwidth at 1 MHz of the transmitted pulse. So, replacing the transmitter with one with smaller diameter and higher frequency might be a solution for this problem.

- iii In Lise's thesis [62] she did some B/A measurements with the National Physics Laboratory (NPL) characterisation system. That system used a different experimental setup for the B/A, specifically they have of an acoustic absorber placed immediately in front of the sample to effectively eliminate the generation of the second harmonic in the water path between the transmitter and the sample, thus making any harmonics detected at the back of the sample arise solely from transit through the sample material. This might be an option worth exploring for future improvements of the system.

5.2.1 Acoustic properties as a function of temperature

Intention of HIFU is to raise the temperature of a selected, isolated tissue volume above 55°C and maintain it for 1 second or longer. A preliminary study was conducted in order to look for the effects of variations in temperature in the acoustic properties of the tissue. Measurements at 38°C and 50°C were conducted for one liver sample and results show:

- i Slightly changes in the attenuation coefficient, particularly at lower frequencies (under 2.5 MHz). Several studies [17][71][63] suggest that attenuation is highly dependent on temperature only above 50°C, that might explain why we don't observe such severe changes.
- ii Speed of sound increased with temperature, this agrees with previous studies [65].
- iii No significant changes in the B/A coefficient. Previous studies show that the values for B/A do increase slightly with temperature [65].

Further work is crucial in order to accurately measure the importance of the temperature in tissue properties.

5.3 Overall conclusions and Future work

To the author's knowledge, this was the first data gathering performed with in vitro preparations of human tissues obtained from a live patient after surgery with an "all-in-one" tissue characterisation system capable of rapidly measuring the acoustic parameters at identical positions in a single sample in a restricted space such as the side room to a hospital operating theatre.

Future work will include:

- Sample protocol improvements, such as sample thickness for example.
- Incorporate the specimen histological data.
- Optimisation of the B/A system.
- Addition of a thermal characterisation system to measure thermal conductivity and specific heat capacity.
- Complete specification of ultrasonic propagation properties of selected tissues and organs, as functions of frequency, temperature, pathological state, etc.

Bibliography

- [1] Osama Al-Bataineh, Jürgen Jenne, and Peter Huber. Clinical and future applications of high intensity focused ultrasound in cancer. *Cancer treatment reviews*, 38(5):346–353, August 2012. PMID: 21924838.
- [2] Osama Al-Bataineh, Jürgen Jenne, and Peter Huber. Clinical and future applications of high intensity focused ultrasound in cancer. *Cancer treatment reviews*, 38(5):346–353, August 2012. PMID: 21924838.
- [3] T. Bakke and T. Gytte. *Ultrasonic Measurement of Sound Velocity in the Pregnant and the Non-Pregnant Cervix Uteri*. August 2009.
- [4] J. C. Bamber and C. R. Hill. Acoustic properties of normal and cancerous human liver—I. dependence on pathological condition. *Ultrasound in Medicine and Biology*, 7(2):121–133, 1981. PMID: 7256971.
- [5] J. C. Bamber, C. R. Hill, and J. A. King. Acoustic properties of normal and cancerous human liver—II dependence on tissue structure. *Ultrasound in Medicine and Biology*, 7(2):135–144, 1981. PMID: 7256972.
- [6] J.C. Bamber and C.R. Hill. Ultrasonic attenuation and propagation speed in mammalian tissues as a function of temperature. *Ultrasound in Medicine & Biology*, 5(2):149–157, 1979.
- [7] Robert Thomas Beyer. *Nonlinear Acoustics*. U.S. Government Printing Office, 1974.
- [8] W. Buschmann, M. Voss, and S. Kemmerling. Acoustic properties of normal human orbit tissues. *Ophthalmic Research*, 1(6):354–364, 1970.
- [9] N. L. Bush, I. Rivens, G. R. ter Haar, and J. C. Bamber. Acoustic properties of lesions generated with an ultrasound therapy system. *Ultrasound in Medicine and Biology*, 19(9):789–801, 1993. PMID: 8134979.

BIBLIOGRAPHY

- [10] J Y Chapelon, J Margonari, Y Theillère, F Gorry, F Vernier, E Blanc, and A Gelet. Effects of high-energy focused ultrasound on kidney tissue in the rat and the dog. *European urology*, 22(2):147–152, 1992. PMID: 1478231.
- [11] J. Y. Chapelon, J. Margonari, F. Vernier, F. Gorry, R. Ecochard, and A. Gelet. In vivo effects of high-intensity ultrasound on prostatic adenocarcinoma dunning r3327. *Cancer Research*, 52(22):6353–6357, November 1992.
- [12] L Chen, I Rivens, G ter Haar, S Riddler, C R Hill, and J P Bensted. Histological changes in rat liver tumours treated with high-intensity focused ultrasound. *Ultrasound in medicine & biology*, 19(1):67–74, 1993. PMID: 8456530.
- [13] L Chen, G ter Haar, C R Hill, S A Eccles, and G Box. Treatment of implanted liver tumors with focused ultrasound. *Ultrasound in medicine & biology*, 24(9):1475–1488, November 1998. PMID: 10385969.
- [14] R C Chivers and R J Parry. Ultrasonic velocity and attenuation in mammalian tissues. *The Journal of the Acoustical Society of America*, 63(3):940–953, March 1978. PMID: 670559.
- [15] R L Clarke, N L Bush, and G R Ter Haar. The changes in acoustic attenuation due to in vitro heating. *Ultrasound in medicine & biology*, 29(1):127–135, January 2003. PMID: 12604124.
- [16] C Damianou and K Hynynen. The effect of various physical parameters on the size and shape of necrosed tissue volume during ultrasound surgery. *The Journal of the Acoustical Society of America*, 95(3):1641–1649, March 1994. PMID: 8176064.
- [17] C A Damianou, N T Sanghvi, F J Fry, and R Maass-Moreno. Dependence of ultrasonic attenuation and absorption in dog soft tissues on temperature and thermal dose. *The Journal of the Acoustical Society of America*, 102(1):628–634, July 1997. PMID: 9228822.
- [18] Subhashish Dasgupta, Janaka Wansapura, Prasanna Hariharan, Ron Pratt, David Witte, Matthew R Myers, and Rupak K Banerjee. HIFU lesion volume as a function of sonication time, as determined by MRI, histology, and computations. *Journal of biomechanical engineering*, 132(8):081005, August 2010. PMID: 20670054.

BIBLIOGRAPHY

- [19] F Dong, E L Madsen, M C MacDonald, and J A Zagzebski. Nonlinearity parameter for tissue-mimicking materials. *Ultrasound in medicine & biology*, 25(5):831–838, June 1999. PMID: 10414900.
- [20] Francis A. Duck. *Physical properties of tissue: a comprehensive reference book*. Academic Press, 1990.
- [21] Francis A Duck. Nonlinear acoustics in diagnostic ultrasound. *Ultrasound in medicine & biology*, 28(1):1–18, January 2002. PMID: 11879947.
- [22] F Dunn, P. D. Edmonds, and W. J. Fry. Absorption and dispersion of ultrasound in biological media. In *Biological Engineering*, page 205–332. McGraw-Hill Book Co., New York, h. p. schwan edition, 1969.
- [23] L A Frizzell. Threshold dosages for damage to mammalian liver by high intensity focused ultrasound. *IEEE transactions on ultrasonics, ferro-electrics, and frequency control*, 35(5):578–581, 1988. PMID: 18290190.
- [24] F J FRY. Precision high intensity focusing ultrasonic machines for surgery. *American journal of physical medicine*, 37(3):152–156, June 1958. PMID: 13545382.
- [25] F J Fry and L K Johnson. Tumor irradiation with intense ultrasound. *Ultrasound in medicine & biology*, 4(4):337–341, 1978. PMID: 753007.
- [26] W. J. Fry and F. J. Fry. Fundamental neurological research and human neurosurgery using intense ultrasound. *IRE Transactions on Medical Electronics*, ME-7(3):166 –181, July 1960.
- [27] W. J. Fry, F. J. Fry, J. W. Barnard, R. F. Krumins, and J. F. Brennan. Ultrasonic lesions in the mammalian central nervous system. *Science*, 122(3168):517–518, September 1955.
- [28] gcochran. *Research Interest*. March 2011.
- [29] M R Gertner, B C Wilson, and M D Sherar. Ultrasound properties of liver tissue during heating. *Ultrasound in medicine & biology*, 23(9):1395–1403, 1997. PMID: 9428138.
- [30] X F Gong, Z M Zhu, T Shi, and J H Huang. Determination of the acoustic nonlinearity parameter in biological media using FAIS and ITD methods. *The Journal of the Acoustical Society of America*, 86(1):1–5, July 1989. PMID: 2754102.

BIBLIOGRAPHY

- [31] S A Goss, R L Johnston, and F Dunn. Comprehensive compilation of empirical ultrasonic properties of mammalian tissues. *The Journal of the Acoustical Society of America*, 64(2):423–457, August 1978. PMID: 361793.
- [32] S.A. Goss and F.J. Fry. The effect of high intensity ultrasonic irradiation on tumor growth. *IEEE Transactions on Sonics and Ultrasonics*, 31(5):491–496, September 1984.
- [33] B Green, R L Bree, H M Goldstein, and C Stanley. Gray scale ultrasound evaluation of hepatic neoplasms: patterns and correlations. *Radiology*, 124(1):203–208, July 1977. PMID: 866640.
- [34] V. A. Del Grosso and C. W. Mader. Speed of sound in pure water. *The Journal of the Acoustical Society of America*, 52(5B):1442–1446, 1972.
- [35] Gail Ter Haar and Constantin Coussios. High intensity focused ultrasound: physical principles and devices. *International journal of hyperthermia: the official journal of European Society for Hyperthermic Oncology, North American Hyperthermia Group*, 23(2):89–104, March 2007. PMID: 17578335.
- [36] Mark F. Hamilton and David T. Blackstock. *Nonlinear Acoustics*. Academic Press, 1998.
- [37] C. R. Hill, J. C. Bamber, and G. R. ter Haar. *Physical Principles of Medical Ultrasonics*. John Wiley & Sons, March 2004.
- [38] C R Hill, I Rivens, M G Vaughan, and G R ter Haar. Lesion development in focused ultrasound surgery: a general model. *Ultrasound in medicine & biology*, 20(3):259–269, 1994. PMID: 8059487.
- [39] C R Hill and G ter Haar. Nonionizing radiation protection. ultrasound. *WHO regional publications. European series*, 25:245–291, 1988. PMID: 3077028.
- [40] K Hynynen and B A Lulu. Hyperthermia in cancer treatment. *Investigative radiology*, 25(7):824–834, July 1990. PMID: 2202694.
- [41] J E Kennedy, G R Ter Haar, and D Cranston. High intensity focused ultrasound: surgery of the future? *The British journal of radiology*, 76(909):590–599, September 2003. PMID: 14500272.

BIBLIOGRAPHY

- [42] J E Kennedy, F Wu, G R ter Haar, F V Gleeson, R R Phillips, M R Middleton, and D Cranston. High-intensity focused ultrasound for the treatment of liver tumours. *Ultrasonics*, 42(1-9):931–935, April 2004. PMID: 15047409.
- [43] James E Kennedy. High-intensity focused ultrasound in the treatment of solid tumours. *Nature reviews. Cancer*, 5(4):321–327, April 2005. PMID: 15776004.
- [44] G Kossoff, E K Fry, and J Jellins. Average velocity of ultrasound in the human female breast. *The Journal of the Acoustical Society of America*, 53(6):1730–1736, June 1973. PMID: 4719257.
- [45] Frederick W. Kremkau. Cancer therapy with ultrasound: A historical review. *Journal of Clinical Ultrasound*, 7(4):287–300, 1979.
- [46] Frederick W. Kremkau, Ralph W. Barnes, and C. Patrick McGraw. Ultrasonic attenuation and propagation speed in normal human brain. *The Journal of the Acoustical Society of America*, 70(1):29–38, 1981.
- [47] Wan-Yee Lau and Eric C H Lai. Hepatocellular carcinoma: current management and recent advances. *Hepatobiliary & pancreatic diseases international: HBPD INT*, 7(3):237–257, June 2008. PMID: 18522878.
- [48] W K Law, L A Frizzell, and F Dunn. Determination of the nonlinearity parameter B/A of biological media. *Ultrasound in medicine & biology*, 11(2):307–318, April 1985. PMID: 4035807.
- [49] Kang Il Lee and Suk Wang Yoon. Prediction of the size of a thermal lesion in soft tissue during HIFU treatment. *Journal of the Korean Physical Society*, 47(4):640–645, 2005.
- [50] Faqi Li, Ruo Feng, Qiang Zhang, Jin Bai, and Zhibiao Wang. Estimation of HIFU induced lesions in vitro: numerical simulation and experiment. *Ultrasonics*, 44 Suppl 1:e337–340, December 2006. PMID: 16908039.
- [51] T Lin, J Ophir, and G Potter. Correlations of sound speed with tissue constituents in normal and diffuse liver disease. *Ultrasonic imaging*, 9(1):29–40, January 1987. PMID: 3299967.
- [52] C A Linke, E L Carstensen, L A Frizzell, A Elbadawi, and C W Fridd. Localized tissue destruction by high-intensity focused ultrasound. *Archives of surgery (Chicago, Ill.: 1960)*, 107(6):887–891, December 1973. PMID: 4751833.

BIBLIOGRAPHY

- [53] John G. Lynn, Raymund L. Zwemer, Arthur J. Chick, and August E. Miller. A new method for the generation and use of focused ultrasound in experimental biology. *The Journal of General Physiology*, 26(2):179–193, November 1942.
- [54] N F Maklad, J Ophir, and V Balsara. Attenuation of ultrasound in normal liver and diffuse liver disease in vivo. *Ultrasonic imaging*, 6(2):117–125, April 1984. PMID: 6539974.
- [55] Wojciech Marczak. Water as a standard in the measurements of speed of sound in liquids. *The Journal of the Acoustical Society of America*, 102(5):2776, 1997.
- [56] Colin R. McArdle. Ultrasonic diagnosis of liver metastases. *Journal of Clinical Ultrasound*, 4(4):265–268, 1976.
- [57] P M Meaney, R L Clarke, G R ter Haar, and I H Rivens. A 3-d finite-element model for computation of temperature profiles and regions of thermal damage during focused ultrasound surgery exposures. *Ultrasound in medicine & biology*, 24(9):1489–1499, November 1998. PMID: 10385970.
- [58] Srikanth Padma, John B Martinie, and David A Iannitti. Liver tumor ablation: percutaneous and open approaches. *Journal of surgical oncology*, 100(8):619–634, December 2009. PMID: 20017157.
- [59] K J Parker, M S Asztely, R M Lerner, E A Schenk, and R C Waag. In-vivo measurements of ultrasound attenuation in normal or diseased liver. *Ultrasound in medicine & biology*, 14(2):127–136, 1988. PMID: 3279691.
- [60] Allison Payne, Urvi Vyas, Adam Blankespoor, Douglas Christensen, and Robert Roemer. Minimisation of HIFU pulse heating and interpulse cooling times. *International journal of hyperthermia: the official journal of European Society for Hyperthermic Oncology, North American Hyperthermia Group*, 26(2):198–208, 2010. PMID: 20146573.
- [61] J. R. Pellam and J. K. Galt. Ultrasonic propagation in liquids: I. application of pulse technique to velocity and absorption measurements at 15 megacycles. *The Journal of Chemical Physics*, 14(10):608, October 1946.

BIBLIOGRAPHY

- [62] L Retat. *Characterisation of the Acoustic, Thermal and Histological Properties of Tissue Required for High Intensity Focused Ultrasound (HIFU) Treatment Planning*. PhD thesis, University of London, 2011.
- [63] M Ribault, J Y Chapelon, D Cathignol, and A Gelet. Differential attenuation imaging for the characterization of high intensity focused ultrasound lesions. *Ultrasonic imaging*, 20(3):160–177, July 1998. PMID: 9921617.
- [64] S A Sapareto and W C Dewey. Thermal dose determination in cancer therapy. *International journal of radiation oncology, biology, physics*, 10(6):787–800, June 1984. PMID: 6547421.
- [65] C M Sehgal, G M Brown, R C Bahn, and J F Greenleaf. Measurement and use of acoustic nonlinearity and sound speed to estimate composition of excised livers. *Ultrasound in medicine & biology*, 12(11):865–874, November 1986. PMID: 3810981.
- [66] Hua-Ping Shen, Jian-Ping Gong, and Guo-Qing Zuo. Role of high-intensity focused ultrasound in treatment of hepatocellular carcinoma. *The American surgeon*, 77(11):1496–1501, November 2011. PMID: 22196664.
- [67] Thomas L. Szabo. *Diagnostic Ultrasound Imaging: Inside Out: Inside Out*. Academic Press, 2004.
- [68] K J Taylor, C A Riely, L Hammers, S Flax, G Weltin, G Garcia-Tsao, H O Conn, R Kuc, and K W Barwick. Quantitative US attenuation in normal liver and in patients with diffuse liver disease: importance of fat. *Radiology*, 160(1):65–71, July 1986. PMID: 3520657.
- [69] K. J. W. Taylor, D. A. Carpenter, C. R. Hill, and V. R. McCready. Gray scale ultrasound imaging the anatomy and pathology of the liver. *Radiology*, 119(2):415–423, January 1976. PMID: 1265273.
- [70] K. J. W. Taylor and C. C. Connolly. Differing hepatic lesions caused by the same dose of ultrasound. *The Journal of Pathology*, 98(4):291–293, 1969.
- [71] U Techavipoo, T Varghese, Q Chen, T A Stiles, J A Zagzebski, and G R Frank. Temperature dependence of ultrasonic propagation speed and attenuation in excised canine liver tissue measured using transmitted and reflected pulses. *The Journal of the Acoustical Society of America*, 115(6):2859–2865, June 2004. PMID: 15237809.

BIBLIOGRAPHY

- [72] U. Techavipoo, T. Varghese, J. A. Zagzebski, T. Stiles, and G. Frank. Temperature dependence of ultrasonic propagation speed and attenuation in canine tissue. *Ultrasonic Imaging*, 24(4):246–260, October 2002. PMID: 12665240.
- [73] G. R. Ter, R. L. Clarke, M. G. Vaughan, and C. R. Hill. Trackless surgery using focused ultrasound: Technique and case report, July 2009.
- [74] G ter Haar, I Rivens, L Chen, and S Riddler. High intensity focused ultrasound for the treatment of rat tumours. *Physics in medicine and biology*, 36(11):1495–1501, November 1991. PMID: 1754620.
- [75] G ter Haar, D Sinnett, and I Rivens. High intensity focused ultrasound—a surgical technique for the treatment of discrete liver tumours. *Physics in medicine and biology*, 34(11):1743–1750, November 1989. PMID: 2685839.
- [76] Rene T Towa, Rita J Miller, Leon A Frizzell, James F Zachary, and Jr O’Brien, William D. Attenuation coefficient and propagation speed estimates of rat and pig intercostal tissue as a function of temperature. *IEEE transactions on ultrasonics, ferroelectrics, and frequency control*, 49(10):1411–1420, October 2002. PMID: 12403142.
- [77] T A Tuthill, R B Baggs, and K J Parker. Liver glycogen and water storage: effect on ultrasound attenuation. *Ultrasound in medicine & biology*, 15(7):621–627, 1989. PMID: 2683289.
- [78] G. E. P. M. van Venrooij. Measurement of ultrasound velocity in human tissue. 1971.
- [79] N I Vykhodtseva, K Hynynen, and C Damianou. Pulse duration and peak intensity during focused ultrasound surgery: theoretical and experimental effects in rabbit brain in vivo. *Ultrasound in medicine & biology*, 20(9):987–1000, 1994. PMID: 7886858.
- [80] Xiu-Jie Wang, Shu-Lan Yuan, Yan-Rong Lu, Jie Zhang, Bo-Tao Liu, Wen-Fu Zeng, Yue-Ming He, and Yu-Rui Fu. Growth inhibition of high-intensity focused ultrasound on hepatic cancer in vivo. *World journal of gastroenterology: WJG*, 11(28):4317–4320, July 2005. PMID: 16038027.
- [81] Zhibiao Wang, Jin Bai, Faqi Li, Yonghong Du, Shuang Wen, Kai Hu, Guihua Xu, Ping Ma, Niangang Yin, Wenzhi Chen, Feng Wu, and Ruo

BIBLIOGRAPHY

- Feng. Study of a "biological focal region" of high-intensity focused ultrasound. *Ultrasound in medicine & biology*, 29(5):749–754, May 2003. PMID: 12754074.
- [82] Peter Neil Temple Wells. *Biomedical ultrasonics*. Academic Press, 1977.
- [83] FRY WJ, MOSBERG WH Jr, BARNARD JW, and FRY FJ. Production of focal destructive lesions in the central nervous system with ultrasound. *Journal of neurosurgery*, 11(5):471, September 1954.
- [84] R.W. Wood and Alfred L. Loomis. XXXVIII. the physical and biological effects of high-frequency sound-waves of great intensity. *Philosophical Magazine Series 7*, 4(22):417–436, 1927.
- [85] A E Worthington, J Trachtenberg, and M D Sherar. Ultrasound properties of human prostate tissue during heating. *Ultrasound in medicine & biology*, 28(10):1311–1318, October 2002. PMID: 12467858.
- [86] B. J. Wuensch, T. F. Hueter, and M. S. Cohen. Ultrasonic absorption in castor oil: Deviations from classical behavior. *The Journal of the Acoustical Society of America*, 28(2):311–312, 1956.
- [87] Guoliang Xu, Guangyu Luo, Longjun He, Jianjun Li, Hongbo Shan, Rong Zhang, Yin Li, Xiaoyan Gao, Shiyong Lin, and Guobao Wang. Follow-up of high-intensity focused ultrasound treatment for patients with hepatocellular carcinoma. *Ultrasound in medicine & biology*, 37(12):1993–1999, December 2011. PMID: 22036638.
- [88] D Zhang and X F Gong. Experimental investigation of the acoustic nonlinearity parameter tomography for excised pathological biological tissues. *Ultrasound in medicine & biology*, 25(4):593–599, May 1999. PMID: 10386735.
- [89] Jian Zhang and Floyd Dunn. In vivo B/A determination in a mammalian organ. *The Journal of the Acoustical Society of America*, 81(5):1635–1637, 1987.

Appendix

Appendix A

Matlab code

A.1 Second harmonic vs. distance data processing

```
1 close all , clear all ;
2 load second_harmonic_characterisation
3 t_vector=zeros(1,26);
4
5 time=data(:,1);
6 harmonic= data(:,2:27);
7 b=zeros(length(time),1);
8 d=zeros(length(time),1);
9 dd=zeros(1,26);
10 p=zeros(1,26);
11
12 a=zeros(625,1);
13
14 figure ;
15 subplot(2,2,1) , plot(time,harmonic(:,1));
16 title('Signal received at the sensor, at z=35mm');
17 xlabel('Time (s)');
18 ylabel('Voltage (mV)');
19
20 for i=1:26
21
22 t_vector(i)=14+((z(1,i)*1000)/cw);
23 t_vector(i)=t_vector(i)*10^(-6);
24
25 b(:,1)=time(:,1)-t_vector(i);
```


APPENDIX A. MATLAB CODE

```
26 d(:,1)= abs(b(:,1));
27 [dd(:,1) p(i)]=min(d(:,1));
28
29 a(:,i)=harmonic(p(i):p(i)+624,i);
30 end
31 subplot(2,2,2), plot(time(p(1):p(1)+624,1),a(:,1));
32 title('10-cycle pulse section of the signal received at
        the sensor, at z=35mm');
33 xlabel('Time (s)');
34 ylabel('Amplitude (mV)');
35
36 sh2=zeros(1,26);
37 sh1=zeros(1,26);
38 L=length(a);
39
40 NFFT=625; % original segment length – the
            % same as the B/A processing routine
41 fs=fs/1000000;
42 f = fs/2*linspace(0,1,NFFT/2+1);
43 Y=zeros(NFFT,26);
44
45 %FFT amplitude of Second Harmonic at z=35mm
46 for i=1:26
47 Y(:,i)=fft(a(:,i),NFFT)/L;
48 sh2(1,i)=abs(Y(11,i));
49 sh1(1,i)=abs(Y(6,i));
50 end
51
52 subplot(2,2,3), plot(f,2*abs(Y(1:NFFT/2+1,1)));
53 title('Frequency spectrum');
54 xlabel('Frequency (MHz)');
55 ylabel('|Y(f)|');
56 axis([0 4 0 0.01]);
57
58 subplot(2,2,4), plot(z,sh2);
59 title('Distance vs FFT amplitude of Second harmonic');
60 xlabel('z (mm)');
61 ylabel('FFT amplitude of Second Harmonic');
62
63 figure, plot(z,sh2);
64 title('Distance vs FFT amplitude of Second harmonic');
```

APPENDIX A. MATLAB CODE

```
65 xlabel( 'z (mm) ');  
66 ylabel( 'FFT amplitude of Second harmonic' );
```